TECHNICAL REPORT STANDARD PAGE

1. Report No.
222

2. Government Accession No.

3. Recipient's Catalog No.

4. Title and Subtitle

Instrumentation of the Red River Bridge
at Boyce, Louisiana

5. Report Date
August 1988

6. Performing Organization Code

7. Author(s)
K. Nam Shiu

8. Performing Organization Report No.
CR-4920 & CR-9649

9. Performing Organization Name and Address

Construction Technology Laboratories, Inc.
5420 Old Orchard Road
Skokie, Illinois 60077-1030

10. Work Unit No.

11. Contract or Grant No.
736-07-18 / 82-3C

12. Sponsoring Agency Name and Address

Louisiana Transportation Research Center
P.O. Box 94245
Baton Rouge, Louisiana 70804-9245

13. Type of Report and Period Covered
Final Report
January 11, 1982 -
June 30, 1988

14. Sponsoring Agency Code
LTRC

15. Supplementary Notes

In cooperation with U.S. Department of Transportation,
Federal Highway Administration

16. Abstract

This report describes the instrumentation program of Red River Bridge at Boyce, Louisiana. The objectives of the program were to measure and evaluate time-dependent deformations, deflections, and temperatures of the Red River Bridge superstructure. To achieve the objectives, field instrumentation was installed on the bridge structure before and during construction. Strain and temperature sensors were placed in three selected bridge segments of one bridge span. Measurements were made for a period of five years.

Concrete physical properties of the instrumented bridge segments were also measured. Measured properties included short-term and long-term properties of concrete cured under controlled laboratory conditions and under an outdoor environment representing the bridge site. Tests were conducted by Louisiana Transportation Research Center personnel. Results were used to evaluate time-dependent and thermal behavior of the Red River Bridge.

Using the actual material design mix, time-dependent analyses of the Red River Bridge during construction were performed. Design construction schedule was used in calculating bridge behavior during construction. Analytical results were then compared with measured strain readings from the instrumented

....continued

17. Key Words

Prestressed concrete, segmental bridges, time-dependent effects, field tests, creep, shrinkage, relaxation, temperature

18. Distribution Statement

No restriction on distribution.

19. Security Classif. (of this report)
Unclassified

20. Security Classif. (of this page)
Unclassified

21. No. of Pages

22. Price

Form DOT F 1700.7 (8-69)

16. Abstract (continued)

bridge segments. Good correlations were obtained between calculated values and measured data.

Long-term bridge deflections and pier rotations were also measured. Measurements provided a record of how the Red River Bridge behaved over a period of five years.

Measurements were also made over four 24-hour periods to determine thermal response due to the diurnal and seasonal temperature variations. Using the measured concrete strains and temperature data, non-linear temperature behavior was confirmed and its effects quantified. Restraint stresses across the three instrumented bridge sections and continuity thermal stresses were calculated. Statistical analyses were performed to evaluate the probability density function of the temperature differentials between top and bottom of the box-girder section. Shear stresses in the webs of the instrumented segments from diurnal temperature changes were calculated. Measured shear strains included continuity shear strains and torsional shear deformations.

INSTRUMENTATION OF THE RED RIVER BRIDGE AT BOYCE, LOUISIANA

FINAL REPORT

By

K. NAM SHIU
Construction Technology Laboratories, Inc.
5420 Old Orchard Road
Skokie, Illinois 60077

Research Project No. 82-36

Conducted for
LOUISIANA DEPARTMENT OF TRANSPORTATION AND DEVELOPMENT
LOUISIANA TRANSPORTATION RESEARCH CENTER
in cooperation with
U.S. DEPARTMENT OF TRANSPORTATION
FEDERAL HIGHWAY ADMINISTRATION

August 1988

Project Nos. CR-4920 & CR-9649 Report Nos. 821-256 through 821-259

ACKNOWLEDGMENTS

This investigation was sponsored by the Louisiana Transportation Research Center (LTRC) and the Federal Highway Administration under State Project No. 736-07-18, Federal Aid Project No. HPR 0010 (005), and Research Project No. 82-3C. Mr. S. C. Shah, Research and Development Engineer of LTRC, and Dr. Ara Arman, Director of LTRC, coordinated the project. Mr. Masood Rasoulian, Concrete Research Engineer of LTRC, implemented all field and laboratory tests and coordinated schedules with Construction Technology Laboratories, Inc. (CTL) and the construction contractor. Their contribution to this investigation is appreciated. Special thanks are also due to Mr. John Gagnard, Field Project Engineer at Boyce, Louisiana, and his staff for their cooperation and assistance in providing access to the instrumented bridge segments as needed.

PROJECT TEAM

RESEARCH EXECUTED BY:	Structural Development Section Structural Engineering Department
RESPONSIBLE EXECUTIVE:	Walter E. Kunze President Construction Technology Laboratories, Inc.
PROJECT MANAGEMENT:	Dr. Henry G. Russell Executive Director Structural Engineering Department
PRINCIPAL INVESTIGATOR:	K. Nam Shiu Senior Engineer Structural Development Section
CO-INVESTIGATOR:	Joseph D. Gilken Senior Engineer Structural Analytical Section
LEAD TECHNICIAN:	Felix R. Gonzales Senior Technician Structural Development Section

TABLE OF CONTENTS

Page

TABLE OF CONTENTS

LIST OF TABLES

LIST OF FIGURES

LIST OF FIGURES

LIST OF FIGURES

LIST OF FIGURES

LIST OF FIGURES

LIST OF FIGURES

LIST OF FIGURES

LIST OF FIGURES

LIST OF FIGURES

LIST OF FIGURES

LIST OF FIGURES

LIST OF FIGURES

INTRODUCTION

In the past decade, segmental concrete construction has been one of the most popular construction methods among U.S. designers and constructors for medium- and long-span bridges. Although segmental concrete construction has been used extensively and successfully in European countries since the early 1950s, post-tensioned, segmental concrete box-girder bridges were introduced into the United States only in the 1970s. With new and innovative concepts in designs, segmental concrete box-girder bridges have become an excellent design alternative in bridge engineering. The construction method offers both aesthetic advantages and economy for bridges in North America.

Because segmental methods of constructing post-tensioned concrete box-girder bridges were relatively new in the United States, design and construction expertise have been primarily adopted from European practices. Specific information on the effects of time-dependent material properties and thermal gradients on bridge performance was needed for American construction. There was also a lack of design provisions and design criteria for segmental box-girder bridges. Consequently, a comprehensive field measurement program of the Red River Bridge at Boyce, Louisiana, was initiated. These measurements reflected behavior of a typical segmental box-girder bridge built in the southern part of the United States. Analyses to evaluate time-dependent and thermal behavior of the bridge were also carried out. Actual concrete mixes of the instrumented bridge segments and design construction schedule were recorded and used in the analyses.

BACKGROUND

In recent years, the long-term behavior of several segmental concrete box-girder bridges in the United States has been investigated. Construction Technology Laboratories, Inc. (CTL) has instrumented six segmental box girder bridges. They are the Denny Creek Bridge (1) in Washington State, the Kishwaukee River Bridge (2 and 3) in Illinois, Linn Cove Viaduct (4) in North Carolina, Sunshine Skyway Bridge in Florida (5, 6), Bayview Bridge in Quincy, Illinois (7), and the Weirton-Steubenville Bridge in West Virginia. Each of these bridges represented a specific type and means of construction. Common objectives for these instrumentation programs were long-term measurements of longitudinal concrete strains and temperature distribution across bridge sections. Of course, specific objectives for each program were different and were reported in detail elsewhere (1-7). With the exception of Denny Creek Bridge, all instrumented bridges were of precast concrete construction. Denny Creek Bridge used cast-in-place, three-stage construction.

In cast-in-place construction, post-tensioning is applied to concrete at a relatively early concrete age. Because concrete creeps and shrinks significantly at early concrete ages, time-dependent behavior for cast-in-place construction is expected to be more significant in long-term bridge behavior than that for precast construction. Consequently, a more in-depth investigation on long-term behavior of cast-in-place bridges was executed.

Instrumentation of the Red River Bridge provided a unique opportunity to obtain actual behavior of a cast-in-place concrete box-girder bridge. Red River Bridge is a long-span, continuous bridge using non-prismatic box segments. The balanced cantilever method of construction with form-travelers was used.

Current design for thermal response of box girders is still based on grossly simplified assumptions (8-10). Little data was available to substantiate the sufficiency of existing code provisions for daily and seasonal temperature cycles. Though a substantial amount of work has been performed overseas on the thermal response of bridges, findings were not necessarily applicable in North American climates without evaluation and verification. In view of the lack of field measurements on thermal response of bridges in North America, it became logical to instrument a long-span, cast-in-place segmental bridge in the southern region of the United States. The Red River Bridge was thus selected. Together with the measured temperature data from other long-span concrete box-girder bridges, collected data on the Red River Bridge has broadened the temperature data base for the development of design provisions for large-span, concrete box girder bridges.

OBJECTIVES AND SCOPE

The objectives of this project were to measure and evaluate time-dependent deformations, deflections, and temperatures of the superstructure of the Red River Bridge in Boyce, Louisiana. Collected data was used to evaluate design criteria for cast-in-place box-girder bridges in the United States.

The investigation was divided into the following parts:

a. Field Instrumentation
b. Material Property Tests
c. Data Analysis and Interpretation
d. Reports

FIELD INSTRUMENTATION

Three cross sections of one selected span in the Red River Bridge were instrumented. Selected sections represented sections next to the pier, at quarter span, and near mid-span. Each section was instrumented to measure longitudinal concrete strains, vertical bridge deflections, and temperature distribution across the box girder. All measuring sensors were installed by CTL personnel. Initial readings of all installed gages were also recorded by CTL. Subsequent readings were taken by field engineers of Louisiana Transportation Research Center (LTRC). Readings were taken before and after every significant event that would affect bridge behavior. Collected field data was sent by LTRC to CTL for data reduction and interpretation.

Effects of temperature variations on bridge performance were investigated. Temperatures and strains of the three instrumented segments were also monitored over four 24-hour periods. The measurements represented the seasonal and diurnal behavior of the bridge.

MATERIAL PROPERTY TESTS

Paralleling the field investigation, laboratory tests were performed on 6x12-in. concrete cylinders. Concrete cylinders were sampled from the same concrete used for each instrumented section. Physical property tests included measurements of concrete compressive strength, modulus of elasticity, Poisson's ratio, coefficient of thermal expansion, creep, and shrinkage. Tests conforming to the appropriate sections of the latest ASTM Specifications were conducted.

Property tests were performed either under controlled, constant laboratory conditions or in the outdoor environment at the bridge site. As such, time-dependent properties of concrete cured under indoor and outdoor conditions were measured. LTRC performed all concrete property tests. Results were collected and sent by LTRC to CTL for analysis.

DATA ANALYSIS AND INTERPRETATION

Long-term, non-linear analysis of the Red River Bridge using the concrete mix properties was performed. Effects of time-dependent properties on bridge performance were investigated. A computer program developed under another investigation was used in the analysis. Time-dependent deformations from concrete creep and shrinkage were calculated. To simulate the conditions of the bridge, a design construction schedule was used in the analytical model. Calculated strains were compared with measured values.

Thermal movements and temperature-induced stresses were calculated. Effects of the induced thermal movements and restraint thermal stresses on bridge behavior were discussed. Thermal effects included longitudinal and transverse temperature movements, nonlinear sectional restraint stresses, and continuity stresses.

REPORTS

An interim report outlining the progress of the investigation was submitted in October, 1985. Collected data and preliminary findings were discussed. In addition, progress reports were submitted quarterly and later biannually to LTRC. This report, which is the final report of the instrumentation program, covers all aspects of the investigation, including data and findings reported earlier. In addition, detailed descriptions of the nonlinear, time-dependent analysis, thermal investigation, and the discussion of measured and analytical results are given. Conclusions drawn from the observed behavior of the Red River Bridge are presented.

DESCRIPTION OF THE RED RIVER BRIDGE

The Red River Bridge shown in Figure 1 is located in Central Louisiana, northeast of Boyce as shown in Figure 2. It is the first concrete, segmental box-girder bridge built in Louisiana. The bridge is made up of six spans with span lengths varying from 228 ft 9 in. to 370 ft. An elevation of the bridge is shown in Figure 3. As the name of the bridge suggests, it spans across the Red River. The total length of the bridge is 1,797 ft 6 in.

The Red River Bridge is a single-cell, non-prismatic, box girder bridge designed to support three traffic lanes. The roadway width of the bridge is 42 ft 10 in. The bridge has haunches at the pier supports. An artist's rendition of the Red River Bridge is shown in Figure 4. The depth of the girder changes from 17 ft 4 in. at the pier supports to 7 ft 4 in. at mid-span.

The Red River Bridge was made up with cast-in-place concrete segments. The length of most bridge segments is 15 ft 8 in.; however, segments next to the pier were generally shorter in length. Maximum segment length was 16 ft 4 in. The balanced cantilever method of construction was used. Form-travelers positioned at the end of the cantilevers were used to facilitate concrete casting. Concrete segments were cast alternatively on each side of the pier cantilevers.

Two pictures of form-travelers sitting at the end of the cantilevers at different stages of construction are shown in Figures 5 and 6. A maximum of four form-travelers were used at one time during construction.

The Red River Bridge was designed in accordance with AASHTO Standard Specifications for Highway Bridges, 1977 (8) and Interim Specifications, 1978 (9), and 1979 (10). Design compressive strength of concrete at 28 days was 5000 psi. The post-tensioning steels used were seven-wire, low-relaxation strands and high-strength Dywidag bars. Design live loads were HS20-44 truck loading or uniform lane loading, whichever governed. A superimposed dead load of 12 psf was included in the design to account for a future wearing surface. Bridge dimensions were designed based on an annual average temperature of 68°F. A linear temperature gradient of 9°F across the depth of the bridge section was used in the design for temperature effects. Time-dependent properties of concrete such as creep and shrinkage were calculated according to FIP-CEB recommendations (11).

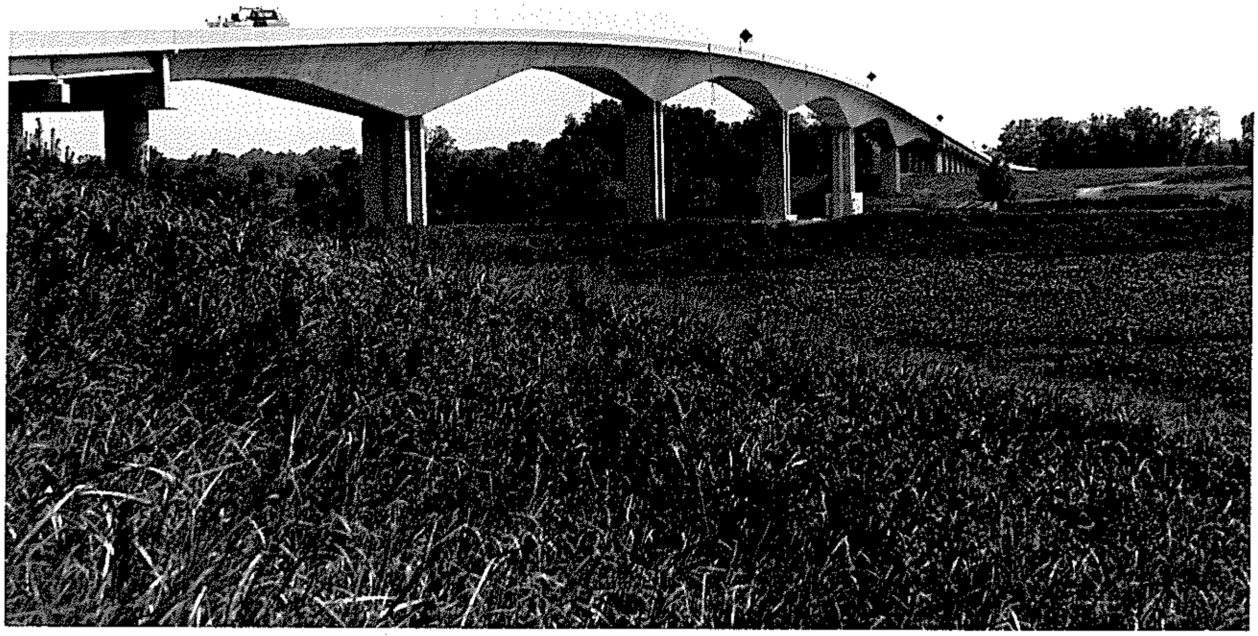

Figure 1. The Red River Bridge.

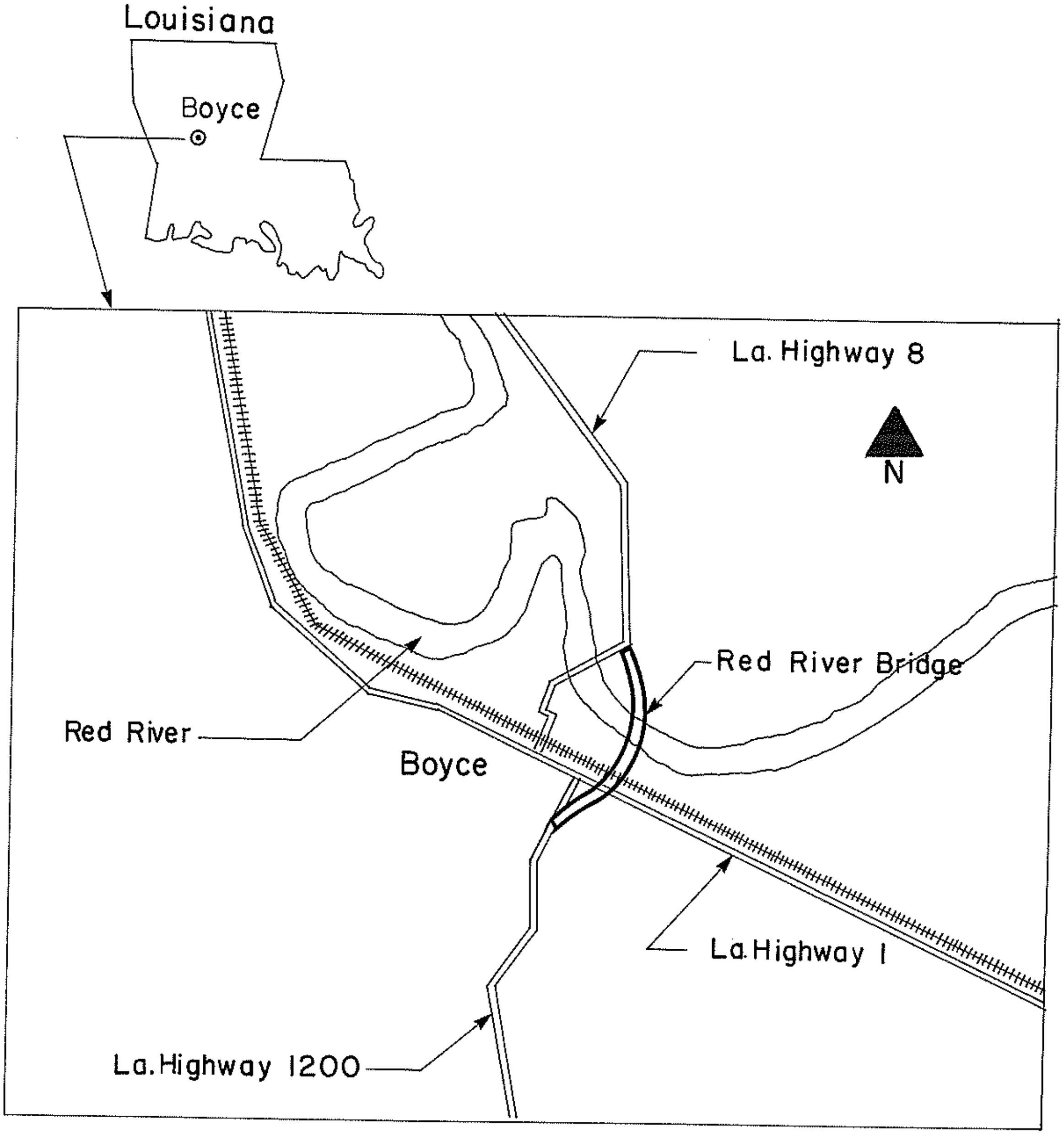

Figure 2. Location of the Red River Bridge.

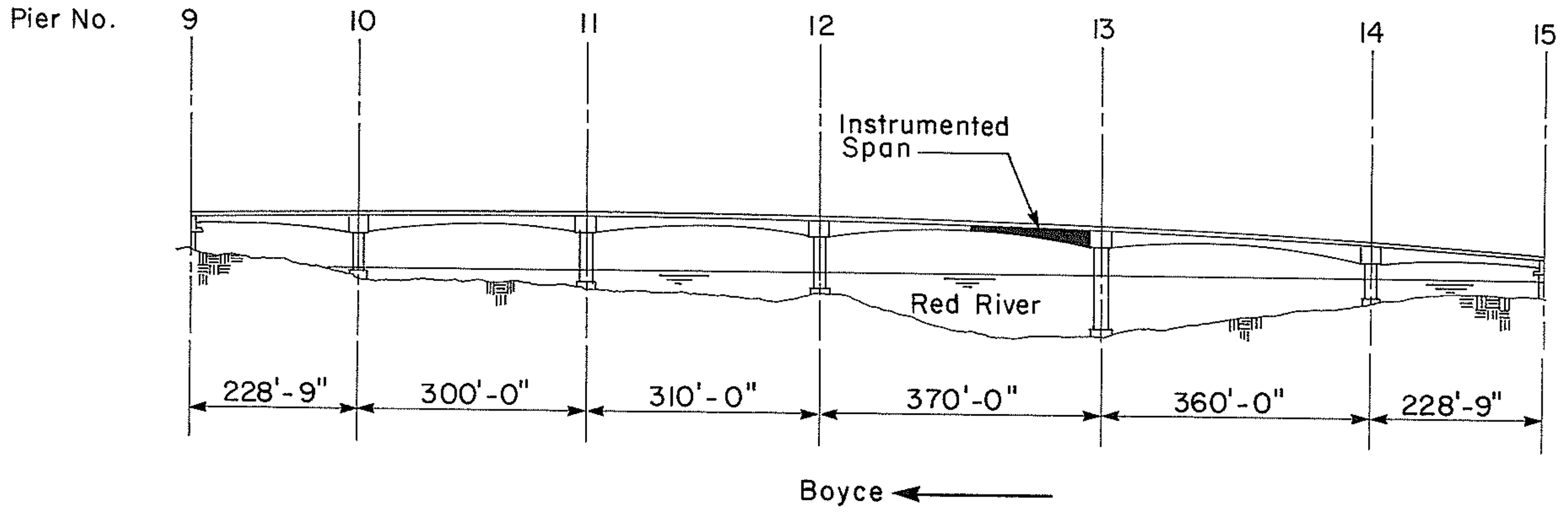

Figure 3. Elevation of the Red River Bridge.

Figure 4. Artist's rendering of the Red River Bridge.

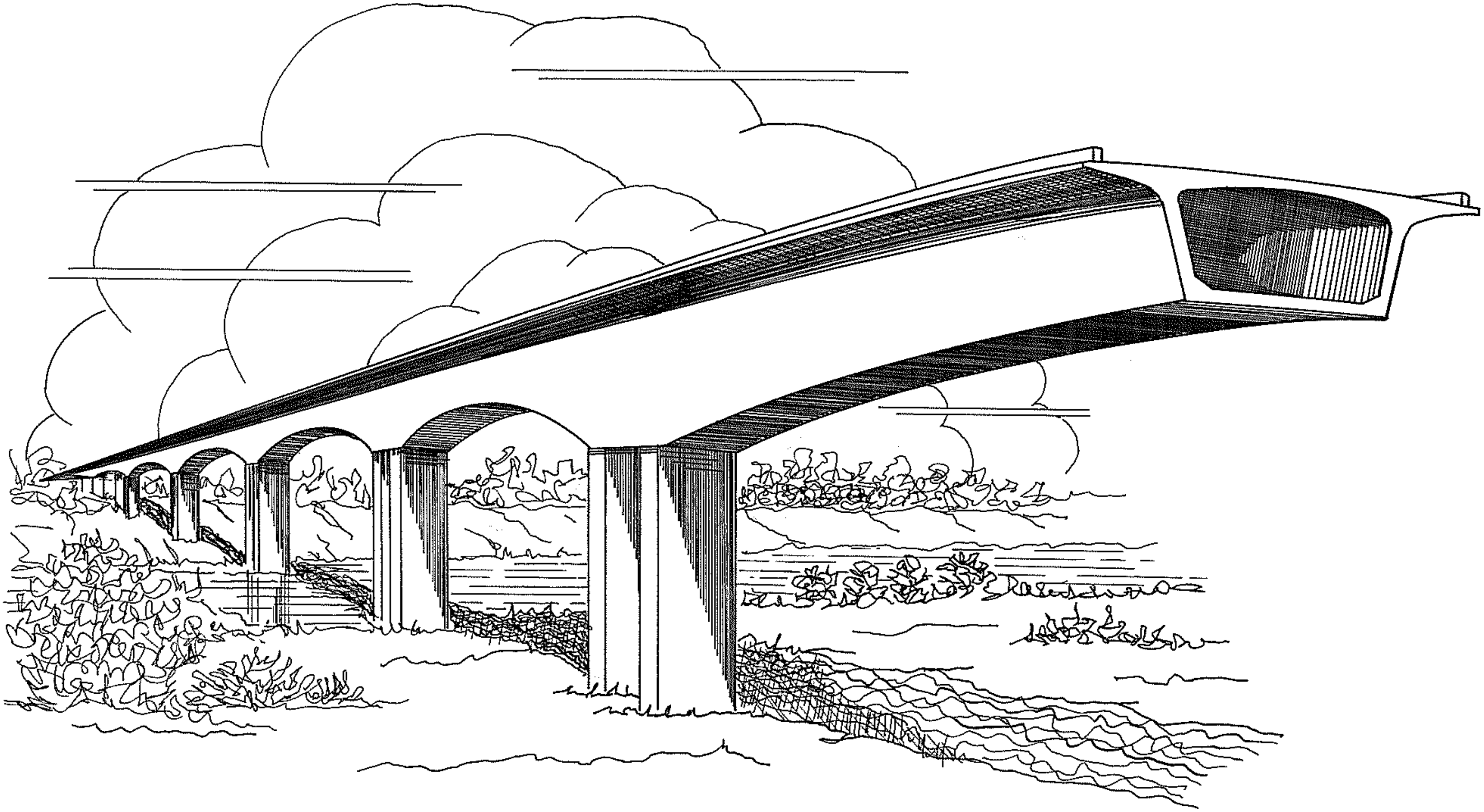

FIG. 3-4 ARTIST'S RENDERING OF THE RED RIVER BRIDGE

Figure 5. A close-up view of form-travelers.

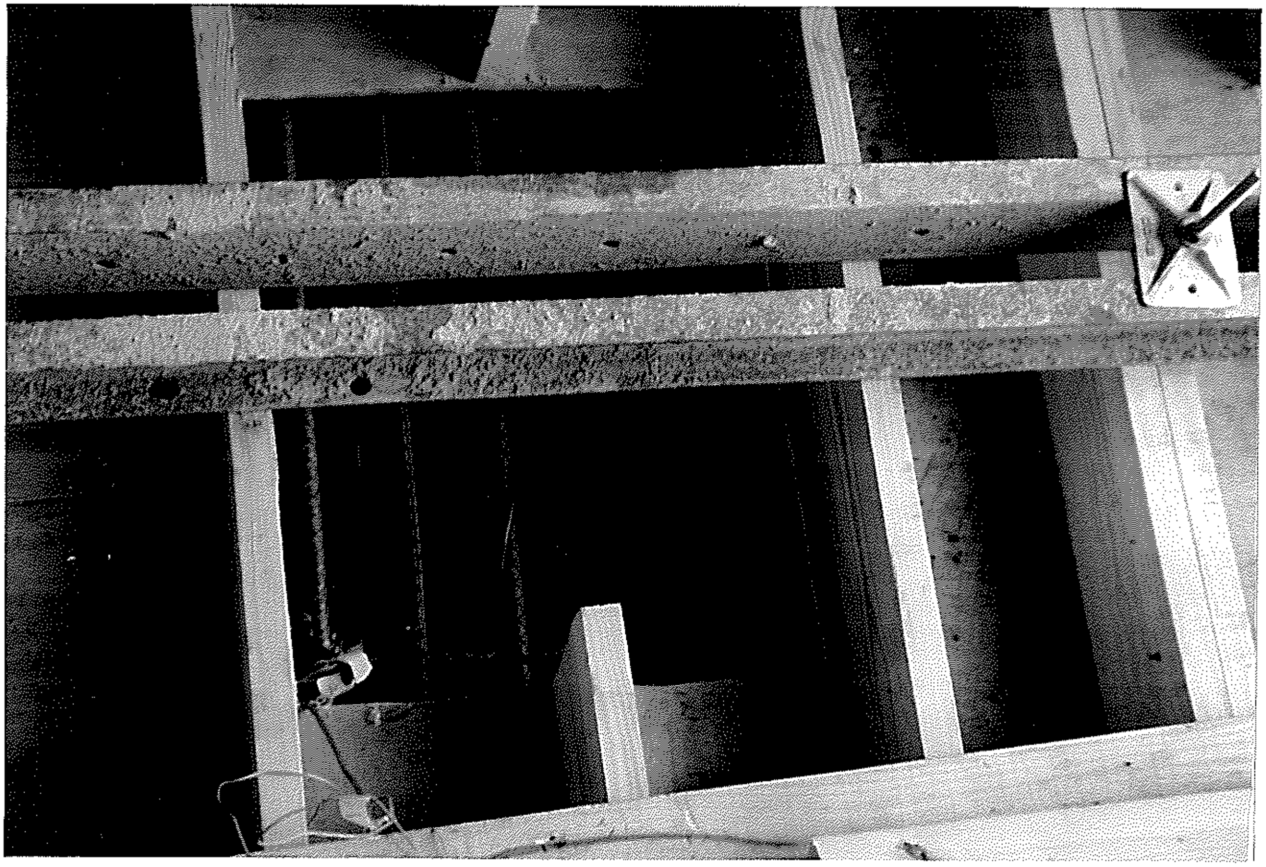

FIG. 4-4 OPENING FOR INSTALLATION OF CARLSON STRAIN METERS IN THE WEB OF THE BOX GIRDER

Figure 11. Installation of Carlson strain meter.

FIG. 4-5 INSTALLATION OF CARLSON STRAIN METER

Figure 12. An installed Carlson strain meter.

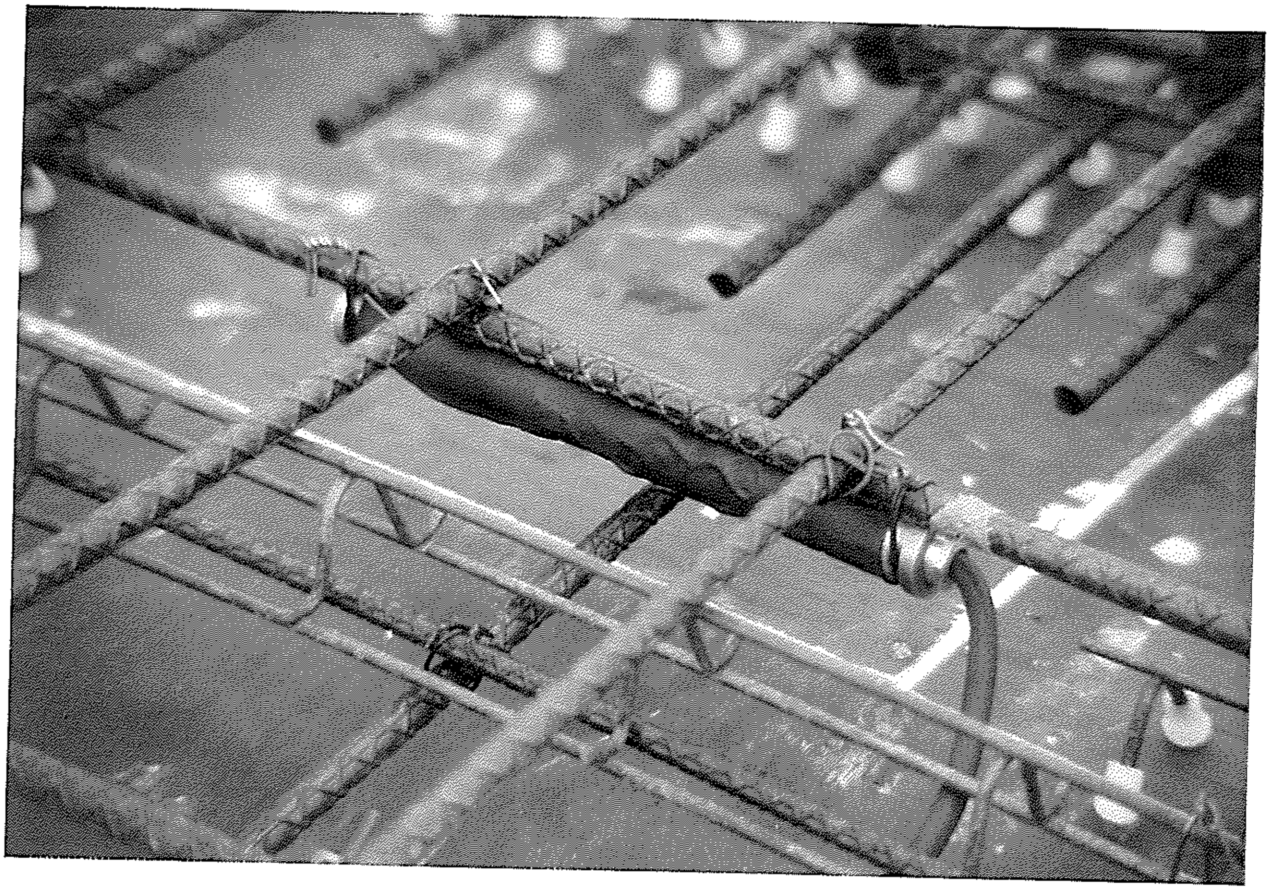

FIG. 4-6 AN INSTALLED CARLSON STRAIN METER

Figure 13. Carlson strain meter lead wire bundle at the bottom slab.

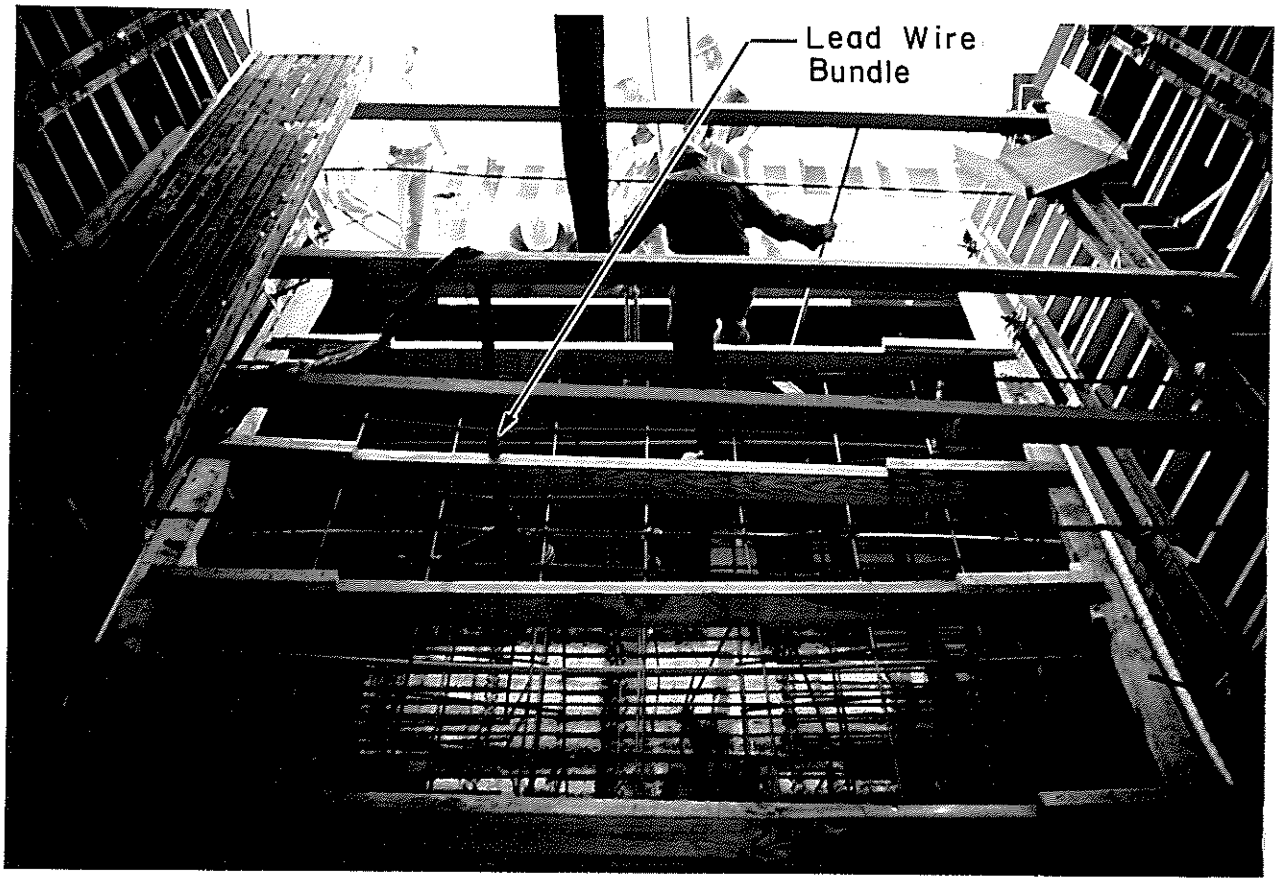

FIG. 4-7 CARLSON STRAIN METER LEAD WIRE BUNDLE AT THE BOTTOM SLAB

Figure 14. Strain rosette.

Relative deflections were calculated using the elevation profile taken on June 28, 1984, or April 3, 1985 as the datum line. It is noted that June 28, 1984, represented the completion of post-tensioning operations in the instrumented span. At that time, the installation of guard railings and the riding roadway overlay was not yet completed. Relative deflections in Table 3 are presented in foot units. Positive relative deflections listed in Table 3 represent downward movements relative to the datum elevation profile, and negative relative deflections indicate upward movements relative to the datum elevation profile. Deflection history of the east deflection point in Segment 1323 is shown in Figure 60. Wide scattering of measured deflections was observed. However, the trend of increasing positive or downward deflection is quite obvious from Figure 60. Maximum downward deflection of 0.9 in. was recorded for the east deflection point on Segment 1323. Deflection profiles of the bridge segments in six different days are shown in Figure 61. Deflections are relative to April 3, 1985 readings.

It is noted that the Segments 1303 and 1304 which were next to the pier support exhibited relative deflections in the order of 0.5 in. This indicates that the pier support column of the bridge moved up vertically relative to the elevation of the pier on April 3, 1985. In addition, the relative deflections of Segments 1303 and 1304 indicated that the pier segment over Pier 13 exhibited a small rotation. This movement was also recorded by the tilt-meter installed on the diaphragm of the pier segment.

Deflection measurements during construction are not presented in this report because those measurements were not always referenced to a fixed bench mark. Consequently, the deflection profile for the bridge cannot be calculated easily. In addition, the accuracy of the recorded elevation readings was to one tenth of a foot. This type of accuracy is satisfactory for construction purposes, but rather crude for long-term monitoring measurements.

ROTATION MEASUREMENTS

Rotation of the pier support is critical in properly evaluating the measured deflection of the instrumented span. Measured rotation readings are presented in Table 4 in arc minutes. An arc minute is one-sixtieth of a degree. Positive rotation in Table 4 represents a clockwise rotation and a

TABLE 4
TILT-METER MEASUREMENTS

Date		Rotation Readings Arc Minutes	Change in Rotation Arc Minutes
6/23/87	12:00 noon	7.19	0
6/24/87	7:15 a.m.	7.12	-0.07
	10:00 a.m.	7.16	-0.03
	1:30 p.m.	7.25	-0.06
6/25/87	2:15 a.m.	7.11	-0.08
	7:00 a.m.	7.12	-0.07
	11:00 a.m.	7.22	-0.03
2/01/88	10:00 a.m.	6.40	-0.79
	1:00 p.m.	6.30	-0.89
	7:00 p.m.	6.35	-0.84
	10:00 p.m.	6.45	-0.74
2/02/88	1:00 a.m.	6.45	-0.74
	4:00 a.m.	6.44	-0.75
	7:00 a.m.	6.36	-0.83
	10:00 a.m.	6.41	-0.78
5/05/88	10:00 a.m.	6.82	-0.37
	1:00 p.m.	6.92	-0.27
	4:00 p.m.	6.95	-0.24
	7:00 p.m.	6.90	-0.29
	10:00 p.m.	6.72	-0.47
5/06/88	1:00 a.m.	6.66	-0.53
	4:00 a.m.	6.64	-0.55
	7:00 a.m.	6.66	-0.53
	10:00 a.m.	6.71	-0.48

negative rotation represents counter-clockwise rotation looking West. It is noted that a rotation change from June 23, 1987, to February 2, 1988, of 0.79 arc minutes represents 0.013 deg. (0.00023 rad.) rotation. A negative change of 0.013 deg. rotation at the pier represented a vertical downward movement of a rigid, non-deflecting cantilever span of 0.50 in. at Segment 1323.

Changes of the Pier 13 rotation within 24-hour periods ranged from 0.15 to 0.31 arc minutes on February 2, 1988, and May 5, 1988, respectively. A change of 0.15 arc minutes represented a vertical movement of a rigid, non-deflecting cantilever span of 0.09 in. at Segment 1323.

24-HOUR MEASUREMENTS

Measurements were made over four 24-hour periods. Data were collected on June 24, 1987, September 23, 1987, February 1, 1988, and May 5, 1988, which represented diurnal behavior of the Red River Bridge in summer, fall, winter, and spring, respectively. In addition, 15-minute-interval temperature readings were taken for 8 hours on August 5, 1986, and for 2 hours on April 1, 1987.

Strain Measurements

On June 24, 1987, strain readings were taken manually at two-hour intervals for 29 hours. Variations of measured strains for the three instrumented Segments 1301, 1313, and 1323 over the 29 hours beginning on June 24, 1987, are shown in Figures 62 through 64, 65 through 67, and 68 through 71, respectively. These measurements provided a record of the daily behavior of the three instrumented bridge segments. For clarity, strain measurements were referenced to the first reading taken at 7:00 a.m. on June 24, 1987. This provides a better presentation of the daily strain fluctuations experienced by the bridge segments. However, with the strain values relative to the 7:00 a.m. readings on June 24, 1987, strain histories of the bridge segment represented only changes of strains since the 7:00 a.m. readings.

Positive strains represent shortening and negative strains represent elongation. Variations of concrete temperatures at the location of the strain gages are also given in each figure. Strains have been adjusted to a reference temperature of 73°F for comparison purposes. Strain adjustments were based on the assumption that thermal movements were totally unrestrained. Measured coefficient of concrete thermal expansion of 6.4 millionths/°F was used. Coefficients of thermal expansion for the strain meters were based on the recommended values provided by the meter manufacturer.

Longitudinal strain variations for the three instrumented bridge Segments 1303, 1313, and 1323 on September 23, 1987, are shown in Figures 72 through 74, 75 through 77, and 78 through 81, respectively. Longitudinal strain measurements for Segments 1303, 1313, and 1323 on February 1, 1988, are given in Figures 82 through 84, 85 through 87, and 88 through 91, and longitudinal strain measurements for Segments 1303, 1313 and 1323 on May 5, 1988 are given in Figures 92 through 94, 95 through 97, 98 through 101, respectively. Please note that strain measurements were not shown in Figures 95 through 97 because no strain measurements for Segment 1313 could be made on May 5, 1988.

Comparisons of the strains in the top and bottom slabs indicated that there was a distinct time lag in the fluctuation of strains between the top and bottom slabs. In addition, the magnitude of strain fluctuation was bigger for the bottom slab strain gages than for the comparable top slab gages. The recorded strain data indicated that the bridge responded to temperature in some form of thermal movements.

It is noted from the figures that concrete strain values changed with the measured concrete temperature. Generally, strain variations were large on June 24, 1987, September 23, 1987, and May 5, 1988. However, relative stable strains were recorded on February 1, 1988. This was also true for the measured concrete temperatures at the concrete strain meter locations.

As expected, the concrete temperature at the top slab of the box girder fluctuated substantially more than that at the bottom slab. As an example, on June 24, 1987, temperature change of 15°F was observed for the top slab of bridge segment 1303, shown in Figure 62 while the bottom slab experienced a temperature fluctuation of only about 4°F.

Temperature Measurements

Measured daily temperature cycles of the instrumented bridge Segments 1303, 1313, and 1323 on August 5, 1986 are presented in Figures 102 through 104, 105 through 107, and 108 through 110, respectively. Distinct temperature cycles were especially observed for the top slab of the box section. However, the temperature fluctuated differently depending on the locations of the thermocouples.

Because one of the surface thermocouples ceased to provide good readings, another thermocouple was connected to that channel to measure inside air temperature. The inside air temperature of the box is plotted in Figure 110. There was a distinct time-lag between the inside box air temperature and the concrete temperatures of the top slab. In addition, comparisons of temperature measurements from Segments 1303 and 1323 indicated that concrete temperatures of bridge Segment 1323 were slightly higher than that at the corresponding locations in Segment 1313 and Segment 1303. Concrete temperatures of the bridge segments tend to be higher as the bridge segments are closer to mid-span. This is contrary to the assumption made by some researchers (13) that there were no longitudinal temperature variations along the bridge axis. The higher recorded temperatures for Segment 1323 were probably due to the smaller sectional depth in Segment 1323 than that in Segments 1303 and 1313.

Similar plots for the daily temperature variation measurements for Segments 1303, 1313, and 1323 on June 24, 1987, September 23, 1987, and February 1, 1988 are presented in Figures 111 throuugh 146. Correlation of the figure numbers, segment locations and gage numbers is given in Table 5.

SHEAR STRAIN MEASUREMENTS

Shear strains were measured in the webs of the instrumented segments. Measurements were taken from three Carlson strain meters in a rosette arrangement. With the relative angle and position of the strain meters, shear deformations can be calculated by the following formulae:

$$\gamma_{xy} = \varepsilon_a + \varepsilon_c - 2\,\varepsilon_b \quad \text{for } \theta_{ab} = 45^\circ \text{ and } \theta_{ac} = 90^\circ \qquad \text{Eq. 5-1}$$

$$\gamma_{xy} = 0.577\,\varepsilon_a + 1.732\,\varepsilon_c - 2.310\,\varepsilon_b \quad \text{for } \theta_{ab} = 60^\circ \text{ and } \theta_{ac} = 90^\circ \qquad \text{Eq. 5-2}$$

where γ_{xy} = Shear Deformation, radian

ε_a = ε_b = ε_c = Measured Strains of the Rosette

θ_{ab} = Angle Between the Horizontal and Diagonal Strain Meters a and b

θ_{ac} = Angle Between the Horizontal and Vertical Strain Meters a and c

TABLE 5
CORRELATION OF FIGURE NUMBERS AND THE DAILY TEMPERATURE PLOTS FOR PLOTS FOR DIFFERENT THERMOCOUPLE LOCATIONS AND SEGMENTS

Figure No.	Date	Segment	Gages
5-86	June 24, 1987	1303	1-5, 6-10
5-87		1303	16-20, 21-25
5-88		1303	26-30
5-89	June 24, 1987	1313	2-5, 6-10
5-90		1313	11-15, 16-20
5-91		1313	21-25, 26-30
5-92	June 24, 1987	1323	1-5, 6-10
5-93		1323	11-15, 16-20
5-94		1323	22-25, 28-30
5-95	September 23, 1987	1303	1-5, 6-10
5-96		1303	16-20, 21-25,
5-97		1303	26-30
5-98	September 23, 1987	1313	1-5, 6-10
5-99		1313	11-15, 16-20
5-100		1313	21-25, 26-30
5-101	September 23, 1987	1323	1-5, 6-10
5-102		1323	11-15, 16-20
5-103		1323	22-25, 28-30
5-104	February 1, 1988	1303	1-5, 6-10
5-105		1303	16-20, 21-25
5-106		1303	26-30
5-107	February 1, 1988	1313	1-5, 6-10
5-108		1313	11-15, 16-20
5-109		1313	21-25, 26-30
5-110	February 1, 1988	1323	1-5, 6-10
5-111		1323	11-15, 16-20
5-112		1323	22-25, 28-30
5-113	May 5, 1988	1303	1-5, 6-10
5-114		1303	12-15, 16-20
5-115		1303	21-25, 26-30
5-116	May 5, 1988	1313	1-5, 6-10
5-117		1313	11-15, 16-20
5-118		1313	21-25, 28-30
5-119	May 5, 1988	1323	1-5, 6-10
5-120		1323	11-15, 16-20
5-121		1323	22-25, 26-30

It is noted that θ_{ab} for Segments 1303 and 1313 was set at 45°. However, due to installation difficulties, θ_{ab} for Segment 1323 was 60°. Shear strain calculations for the three segments were based on the appropriate equations above.

With the sign convention of positive strain representing compressive movements, positive shear strains γ_{xy} represent a decrease of shear angle between the horizontal and vertical axis and negative shear strains γ_{xy} represent an increase of the shear angle.

Measured shear strain histories of the Segments 1303, 1313, and 1323 are shown in Figures 147, 148, and 149, respectively. Shear strains were calculated for both the east and west web of the box girder. It is noted that a big increase of shear strains was observed at age 395 days on Segment 1303, age 240 days on Segment 1313, and age 152 days on Segment 1323. The ages of these three segments represented the readings taken on October 17, 1984, when the guardrail and roadway overlay was installed. Consistently in the three segments, the east web of the instrumented segments registered an increase of shear strains while the west web exhibited a decrease in shear strains. Not knowing the exact loading conditions of the bridge on October 17, 1984, it was virtually impossible to find an explanation for the changes in shear strain. However, subsequent shear strains indicated a stabilized strain history.

It is noted from Figures 147, 148, and 149 that the magnitude of shear strain increases measured at Segment 1303 before the installation of guard railing were larger than that in Segment 1313 and Segment 1323. Segment 1303 was located next to the pier. Before the closing of the mid-span segment, the span segments were in a balanced cantilever condition. Consequently, Segment 1303 experienced a higher dead weight-induced shear stress than those segments closer to the end of the free cantilever.

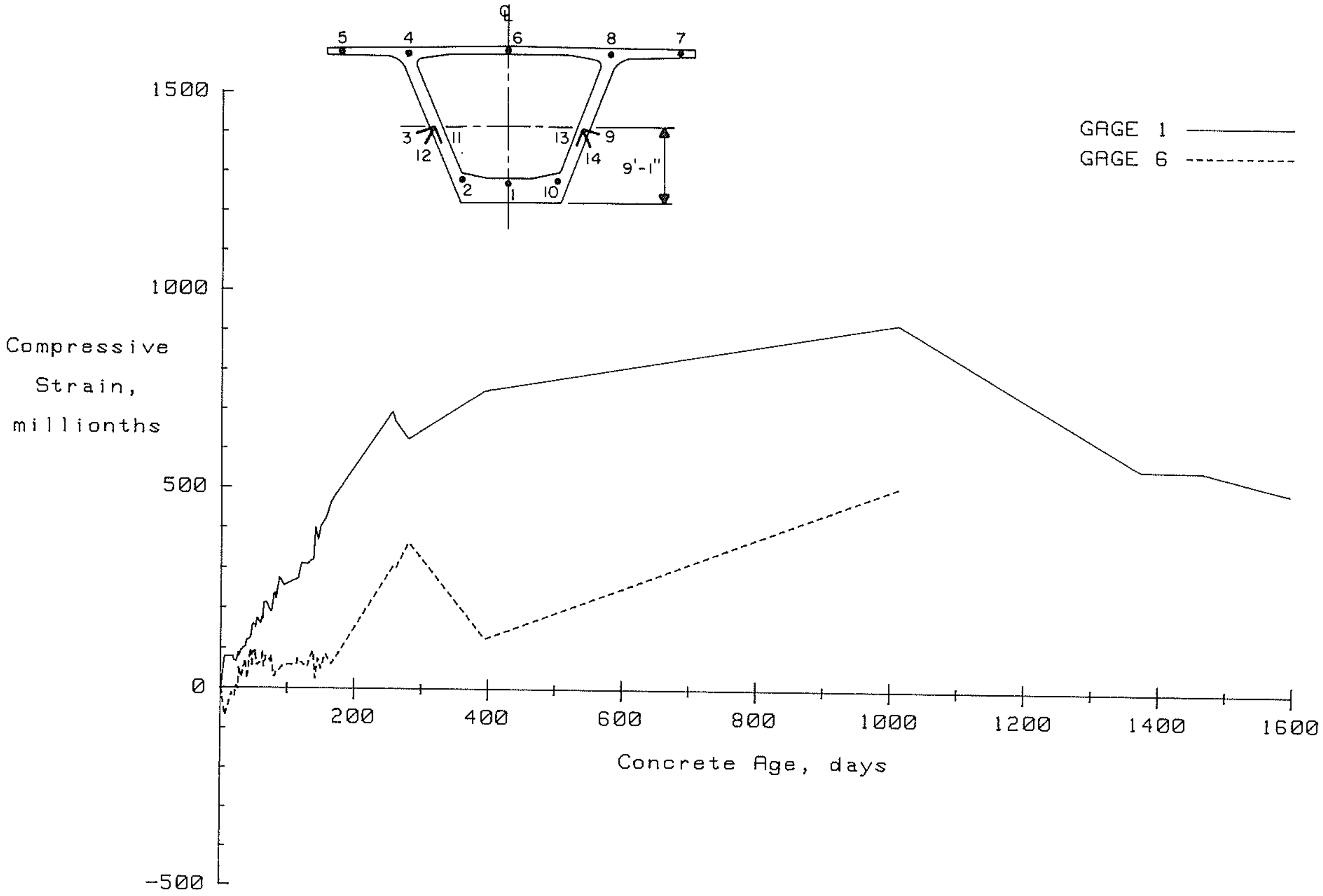

FIG. 5-1 CARLSON STRAIN DATA FOR GAGES 1 AND 6 OF SEGMENT 1303

Figure 26. Carlson strain data for Gages 1 and 6 of Segment 1303.

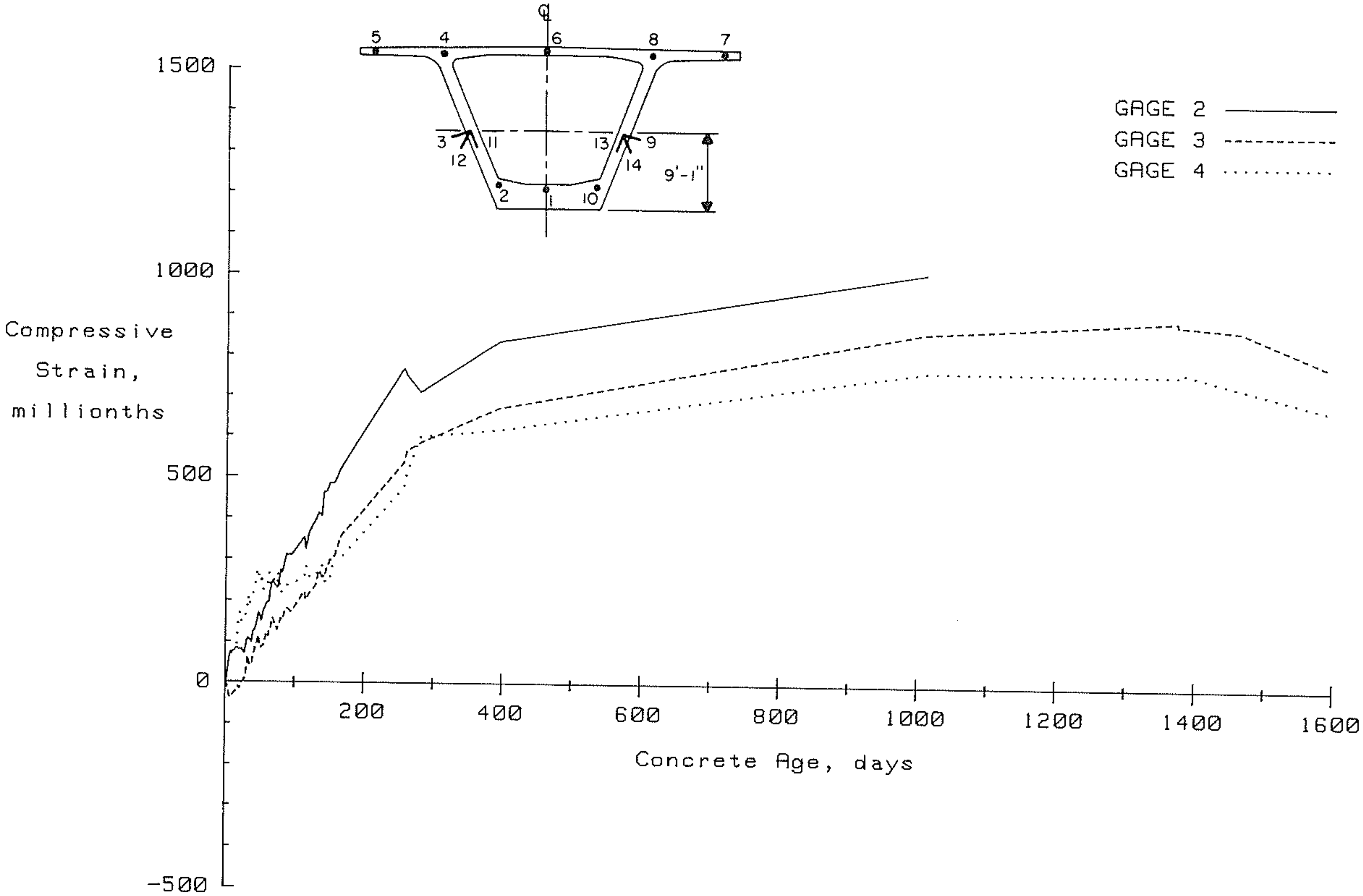

FIG. 5-2 CARLSON STRAIN DATA FOR GAGES 2, 3, AND 4 OF SEGMENT 1303

Figure 27. Carlson strain data for Gages 2, 3, and 4 of Segment 1303.

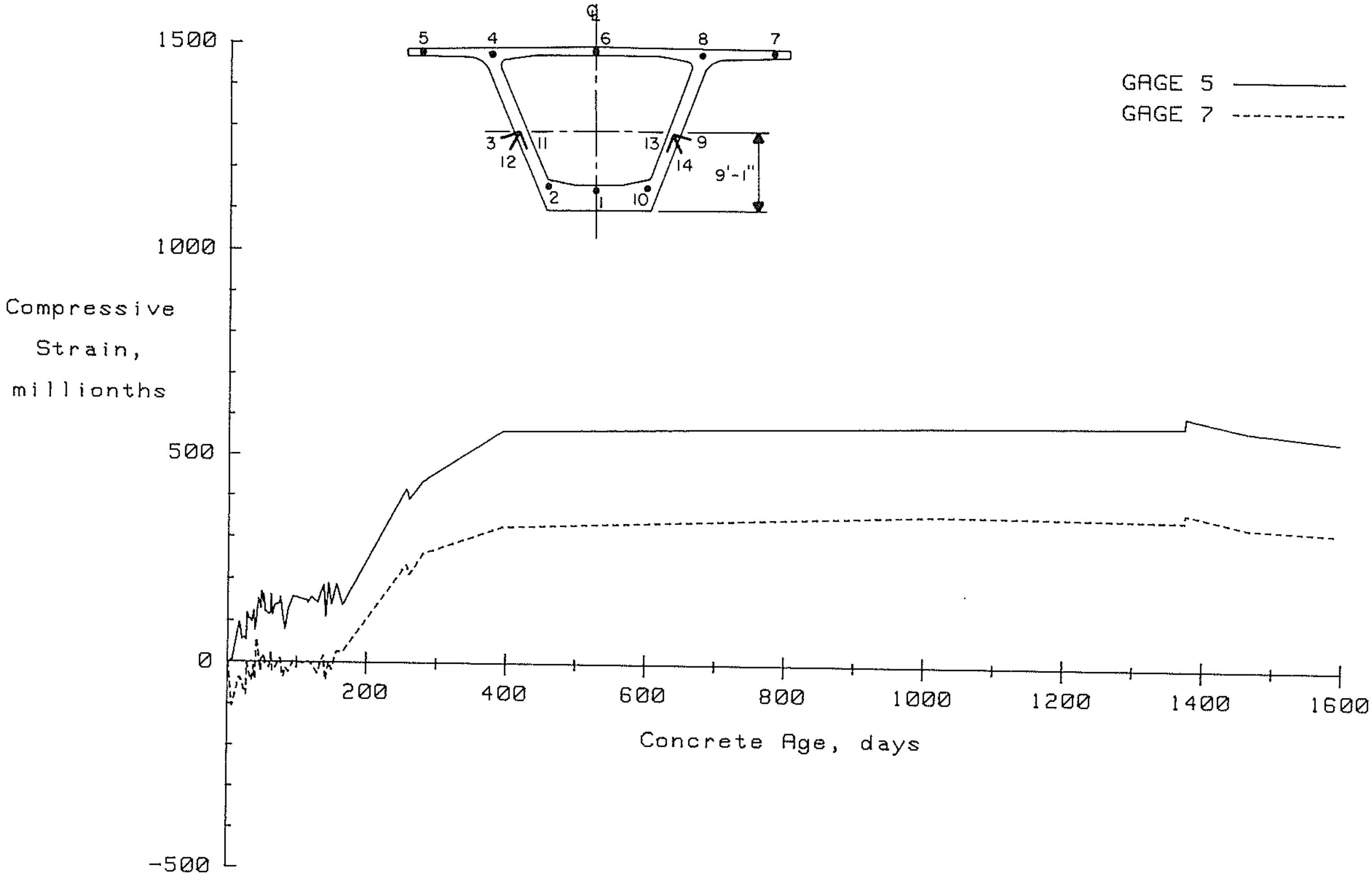

FIG. 5-3 CARLSON STRAIN DATA FOR GAGES 5 AND 7 OF SEGMENT 1303

Figure 28. Carlson strain data for Gages 5 and 7 of Segment 1303.

Figure 18. Locations of deflection measurement points for Segments 1303, 1313, and 1323.

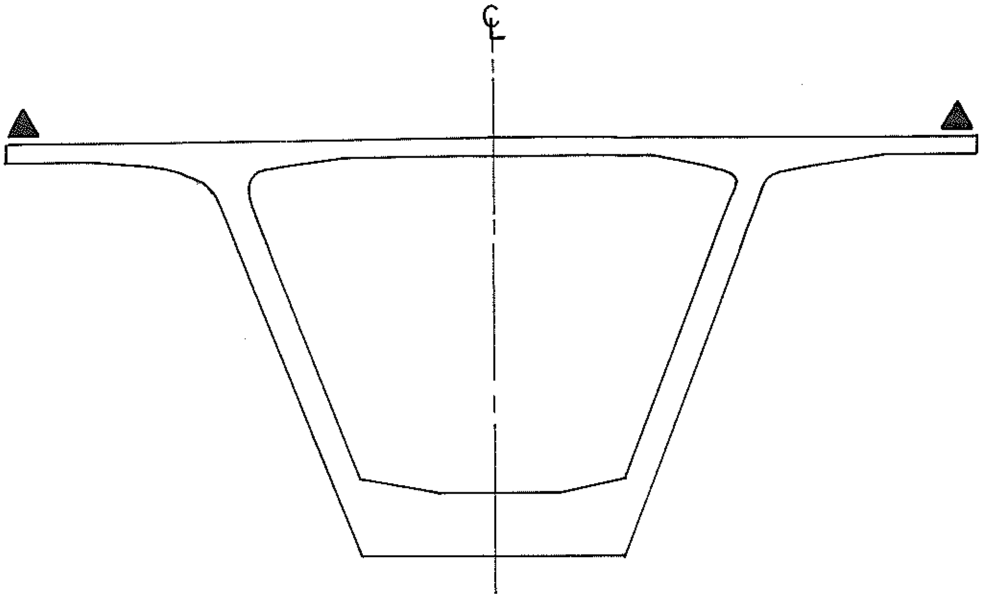

a) Segment 1303

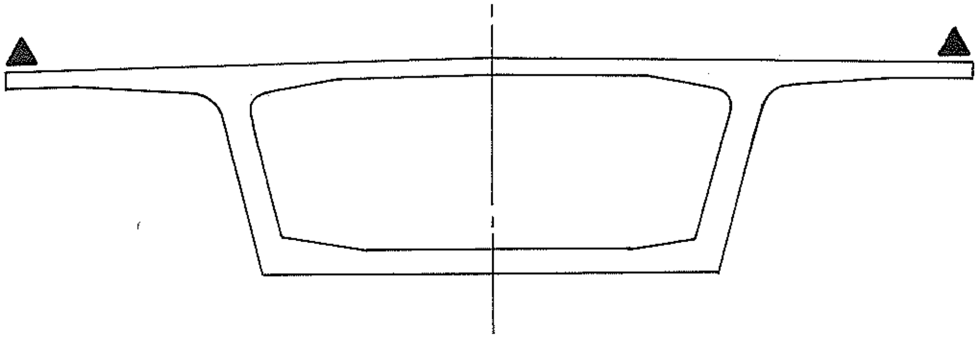

b) Segment 1313

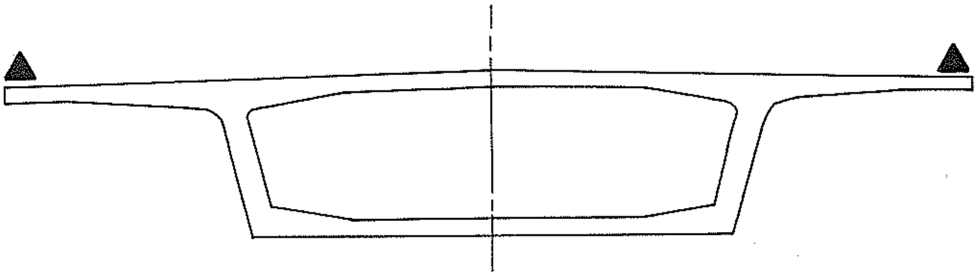

c) Segment 1323

FIG. 4-12 LOCATIONS OF DEFLECTION MEASUREMENT POINTS FOR SEGMENTS 1303, 1313, and 1323

Figure 19. Installed deflection measurement point.

FIG. 4-13 INSTALLED DEFLECTION MEASUREMENT POINT

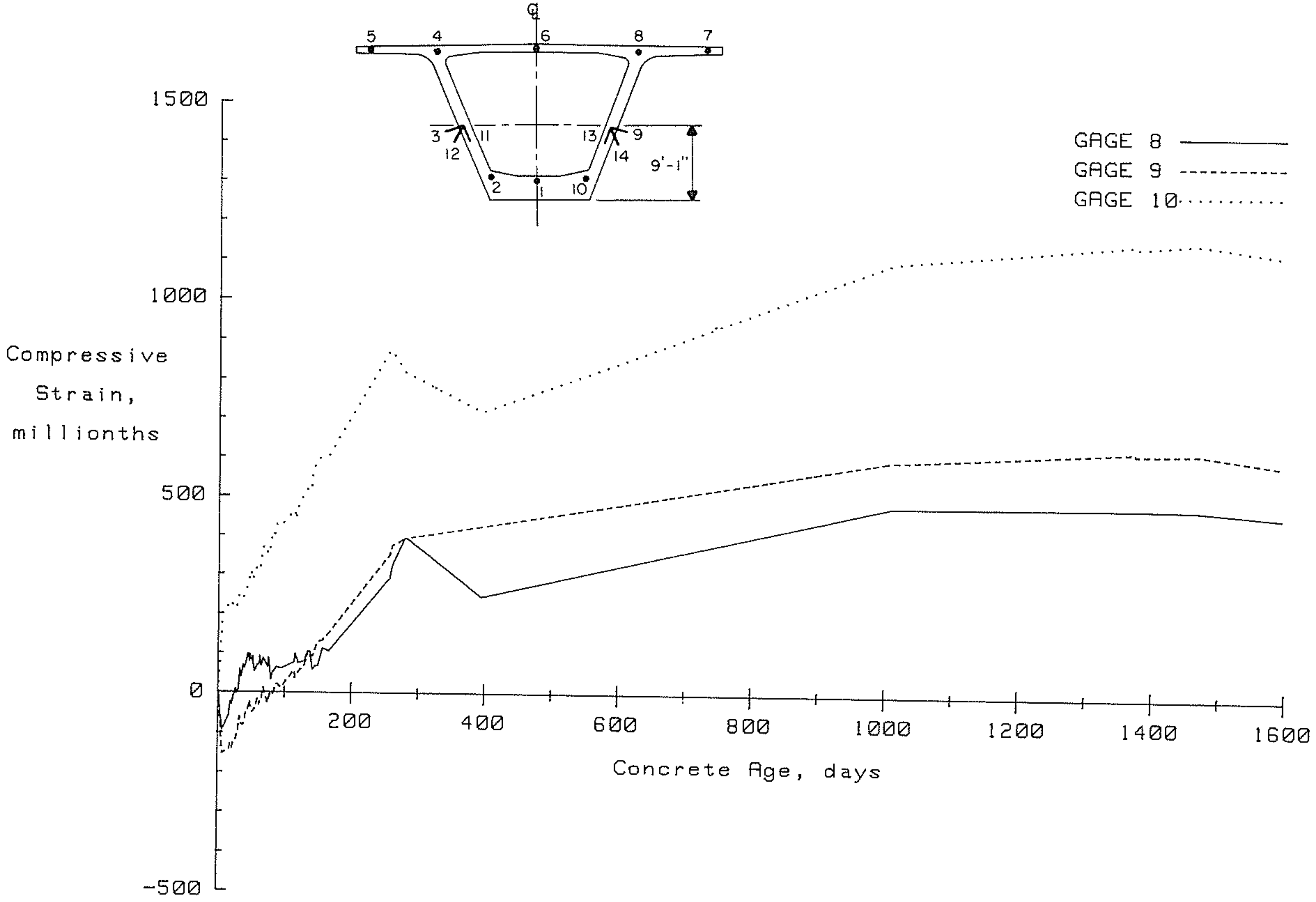

FIG. 5-4 CARLSON STRAIN DATA FOR GAGES 8, 9, AND 10 OF SEGMENT 1303

Figure 29. Carlson strain data for Gages 8, 9, and 10 of Segment 1303.

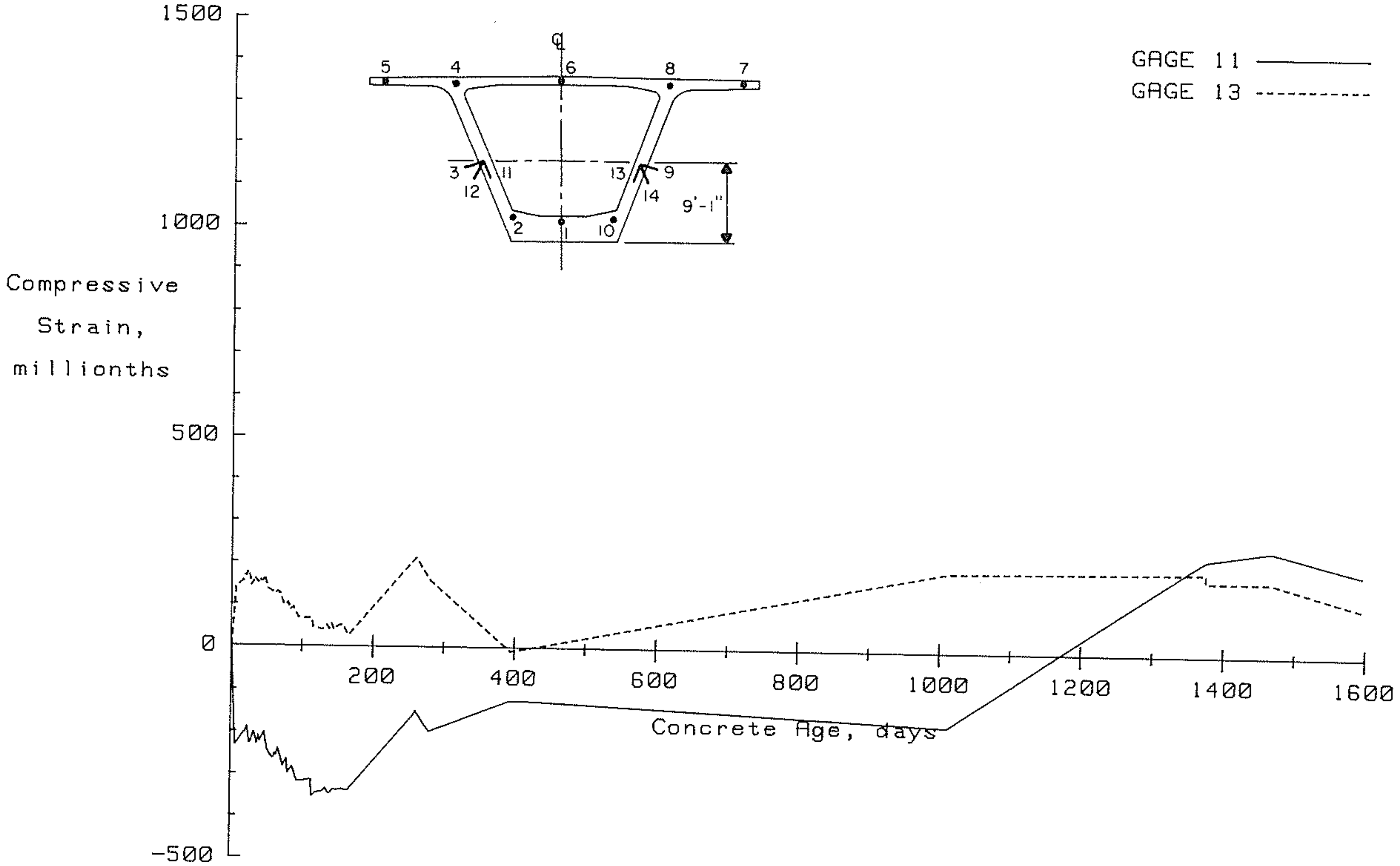

FIG. 5-5 CARLSON STRAIN DATA FOR GAGES 11 AND 13 OF SEGMENT 1303

Figure 30. Carlson strain data for Gages 11 and 13 of Segment 1303.

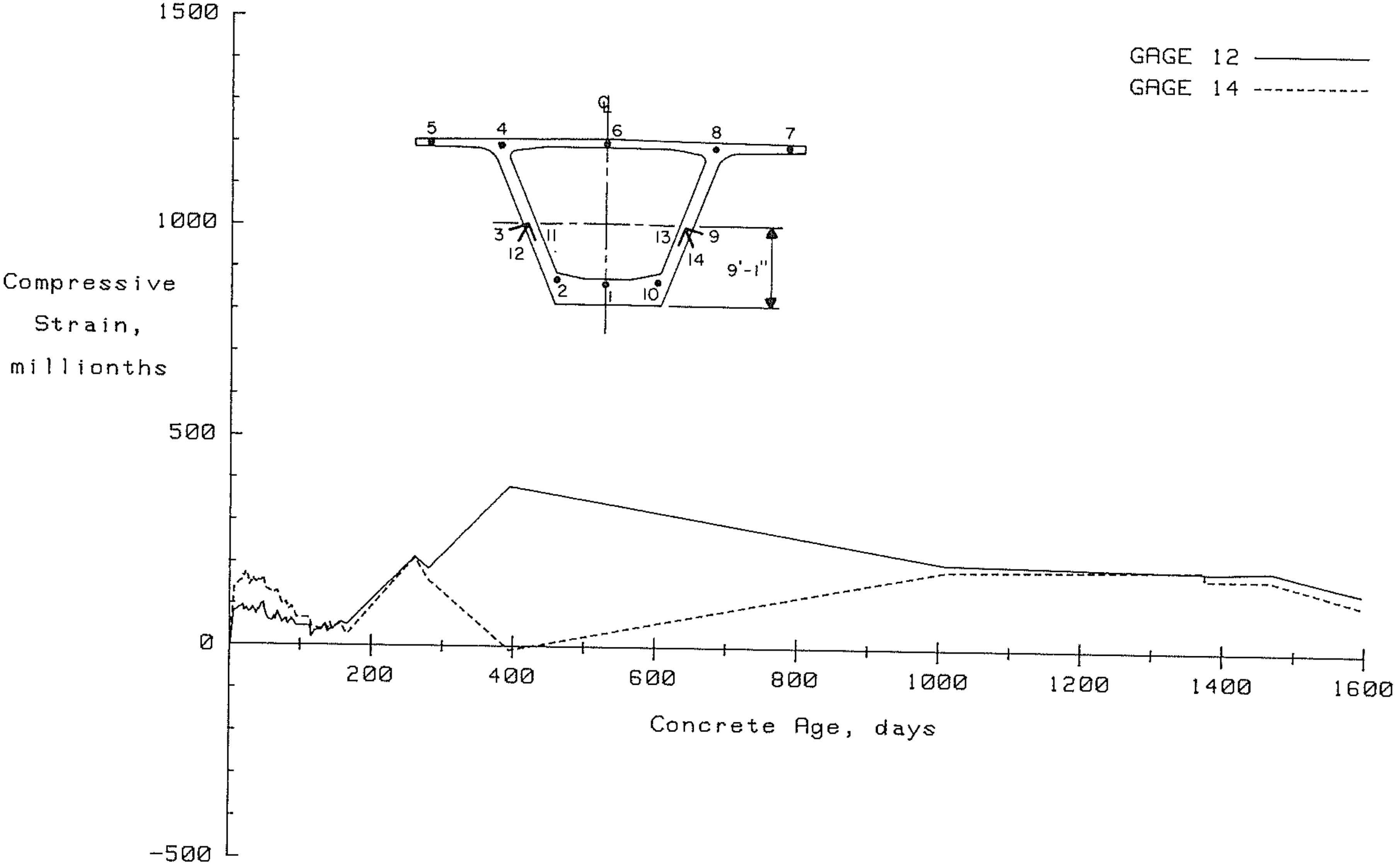

FIG. 5-6 CARLSON STRAIN DATA FOR GAGES 12 AND 14 OF SEGMENT 1303

Figure 31. Carlson strain data for Gages 12 and 14 of Segment 1303.

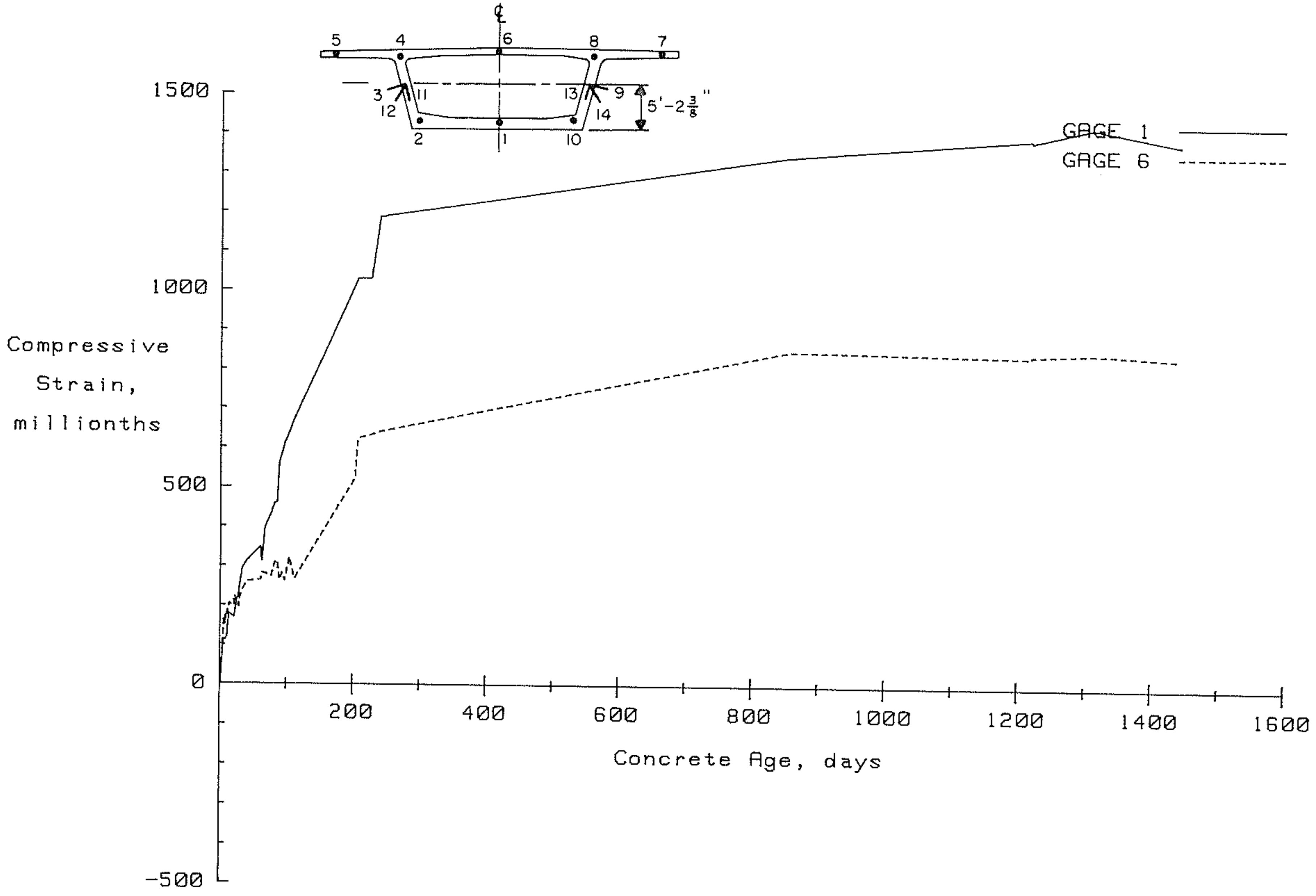

FIG. 5-7 CARLSON STRAIN DATA FOR GAGES 1 AND 6 OF SEGMENT 1313

Figure 32. Carlson strain data for Gages 1 and 6 of Segment 1313.

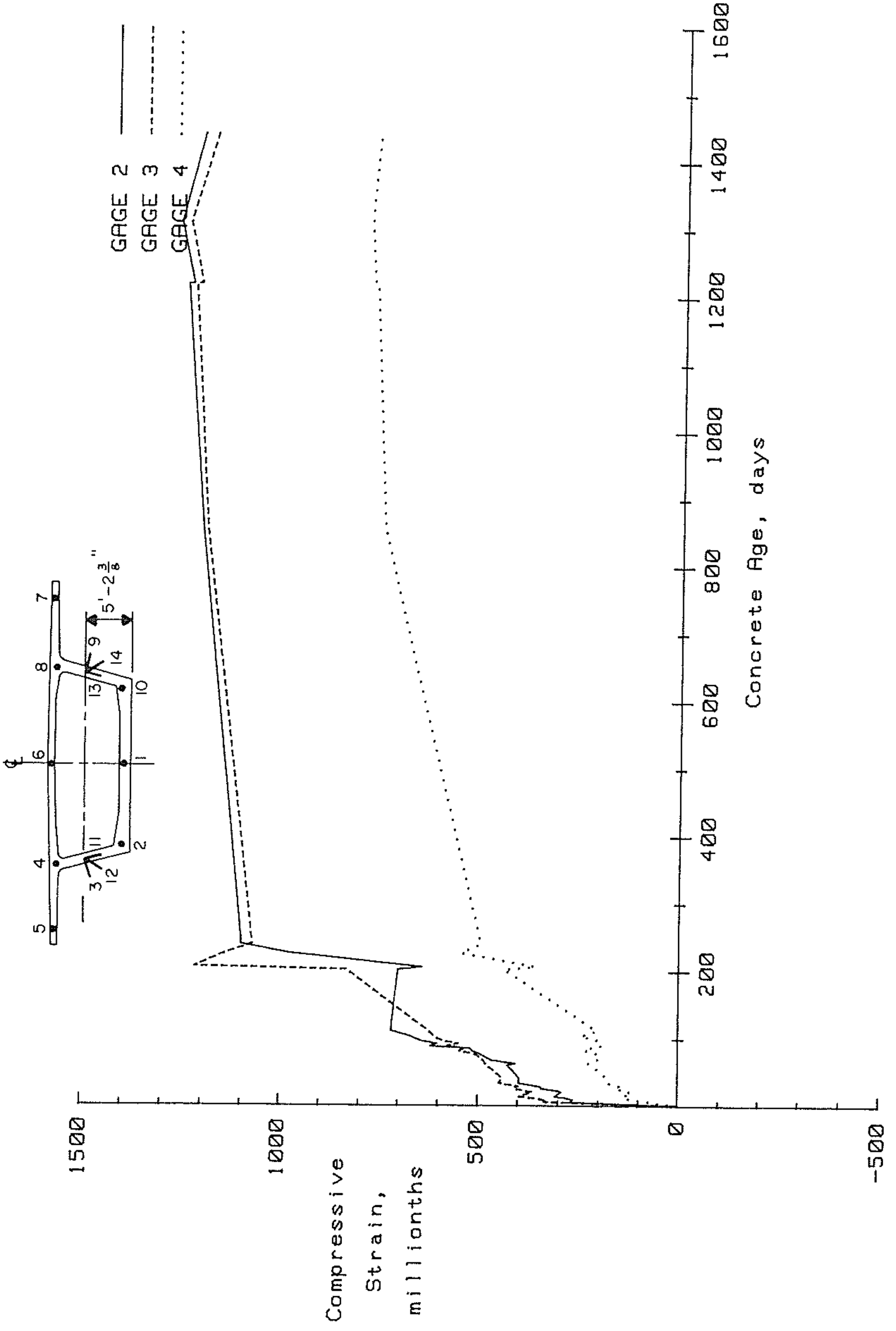

FIG. 5-8 CARLSON STRAIN DATA FOR GAGES 2, 3, AND 4 OF SEGMENT 1313

Figure 33. Carlson strain data for Gages 2, 3, and 4 of Segment 1313.

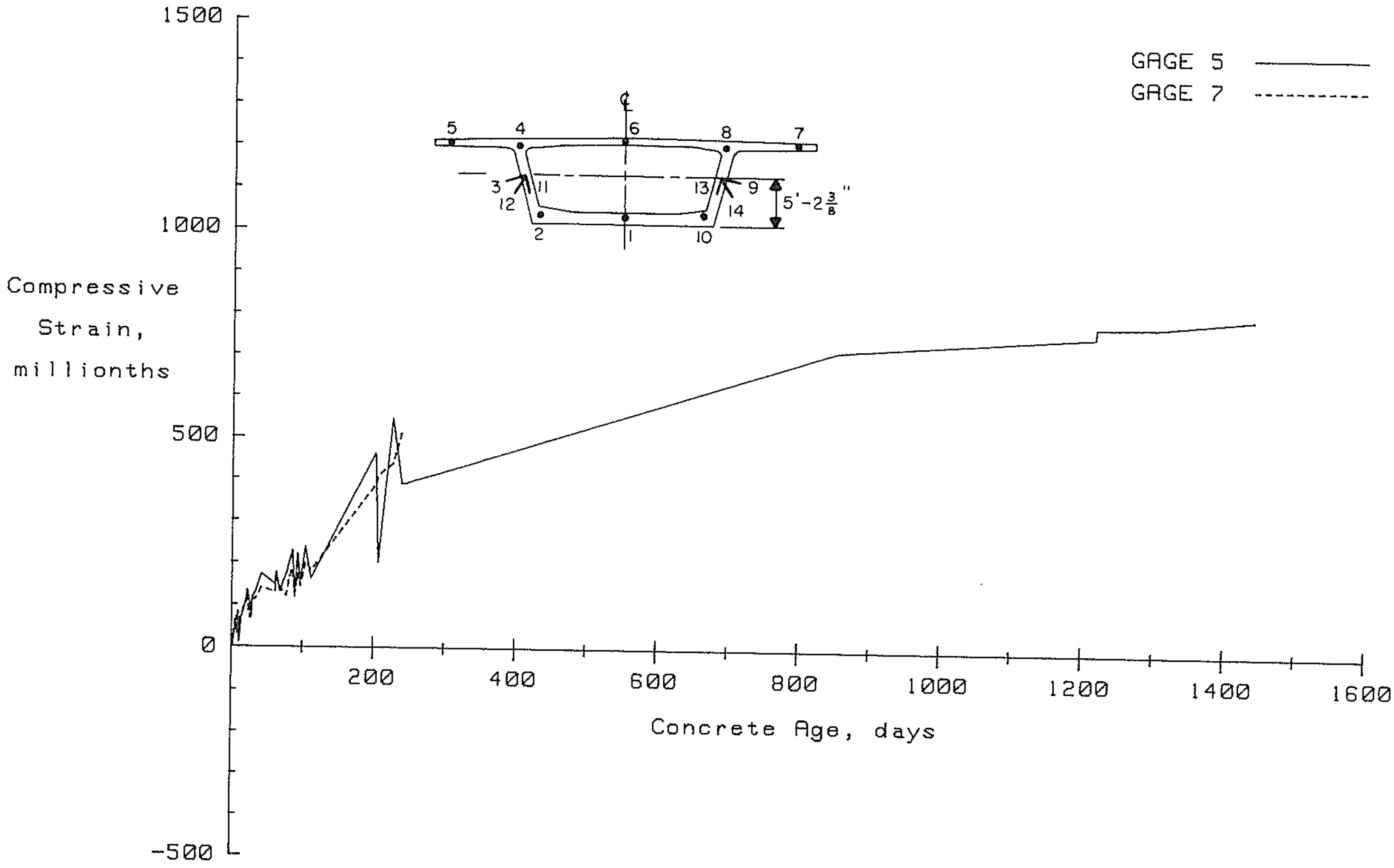

FIG. 5-9 CARLSON STRAIN DATA FOR GAGES 5 AND 7 OF SEGMENT 1313

Figure 34. Carlson strain data for Gages 5 and 7 of Segment 1313.

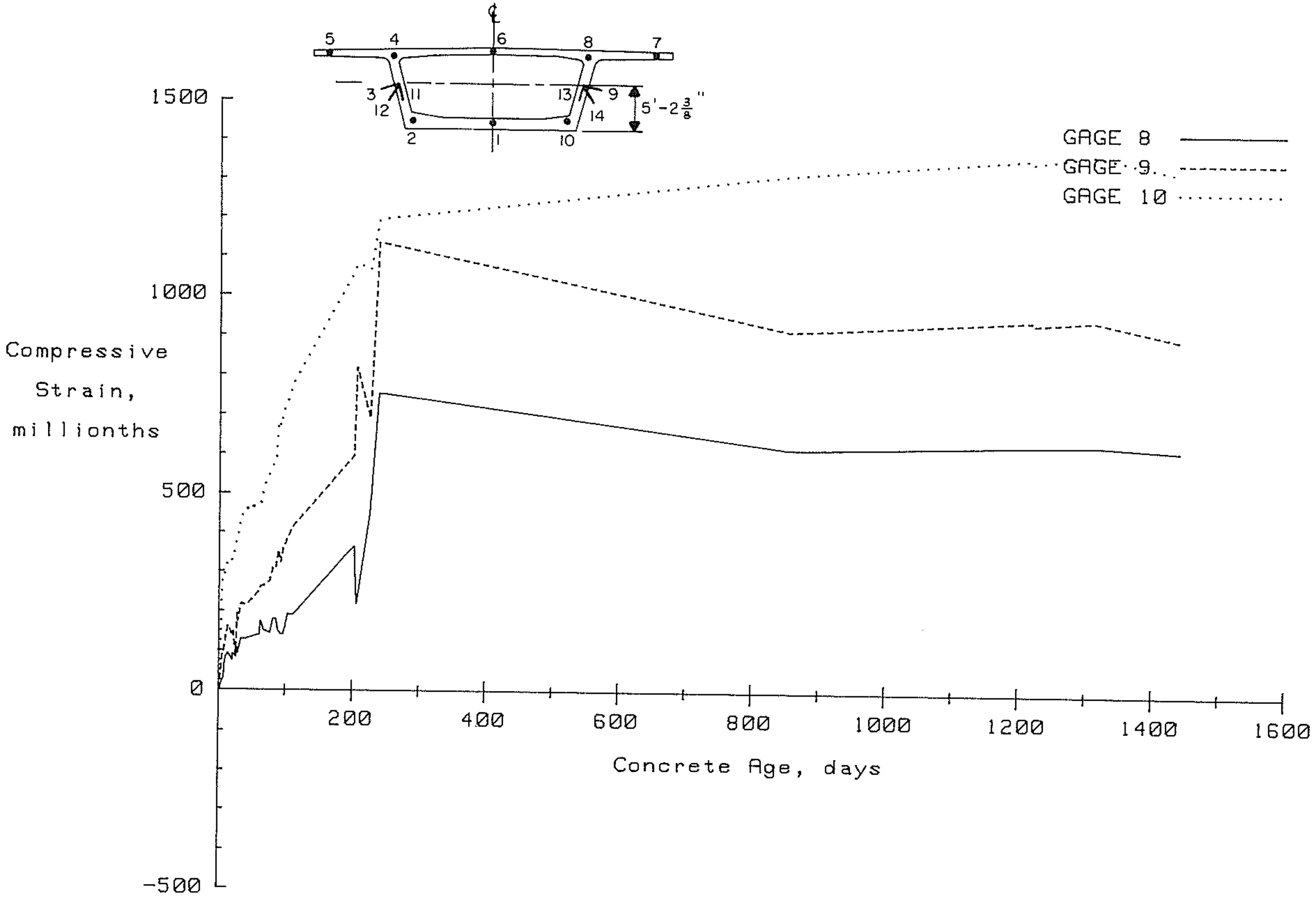

FIG. 5-10 CARLSON STRAIN DATA FOR GAGES 8, 9, AND 10 OF SEGMENT 1313

Figure 35. Carlson strain data for Gages 8, 9, and 10 of Segment 1313.

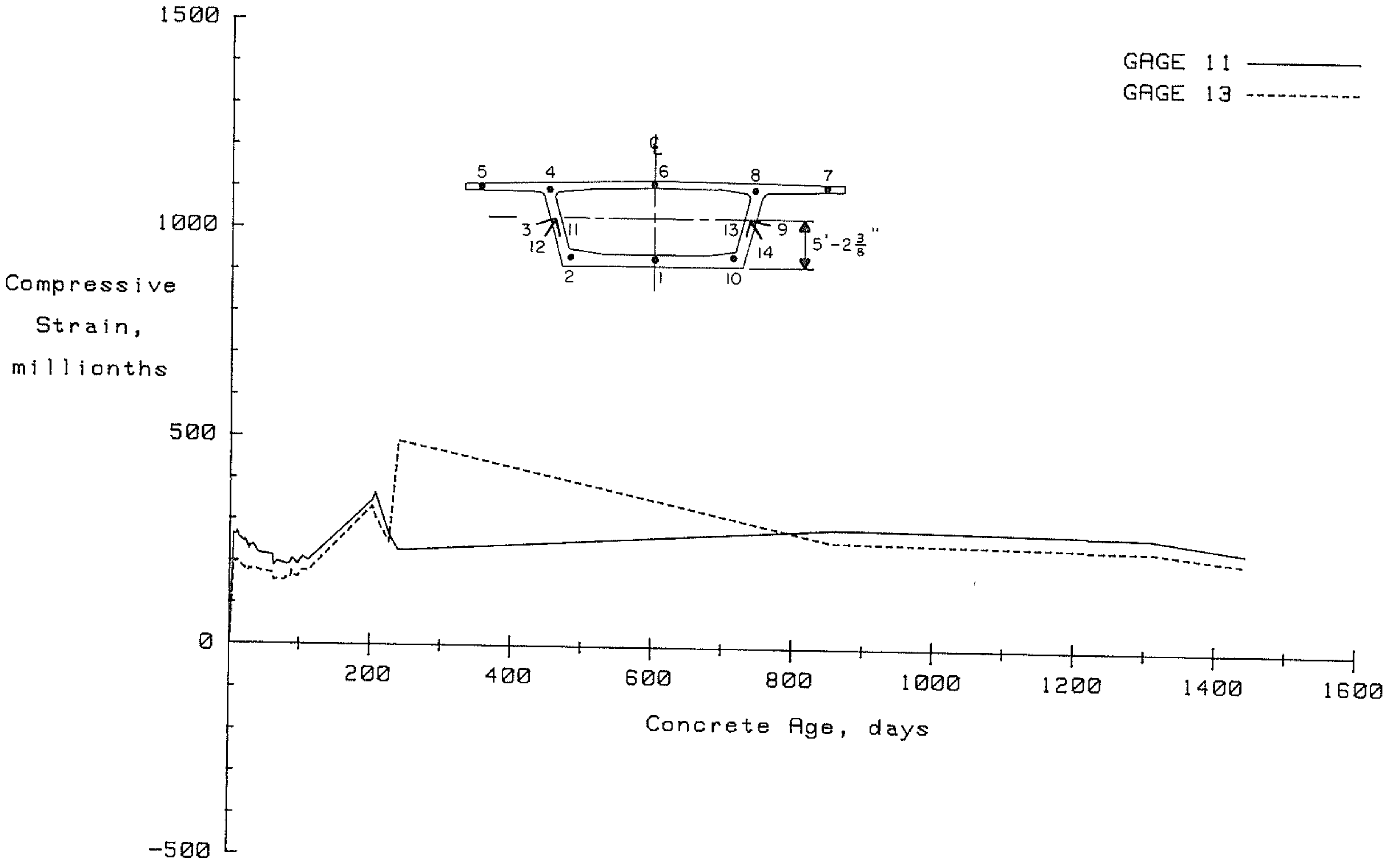

FIG. 5-11 CARLSON STRAIN DATA FOR GAGES 11 AND 13 OF SEGMENT 1313

Figure 36. Carlson strain data for Gages 11 and 13 of Segment 1313.

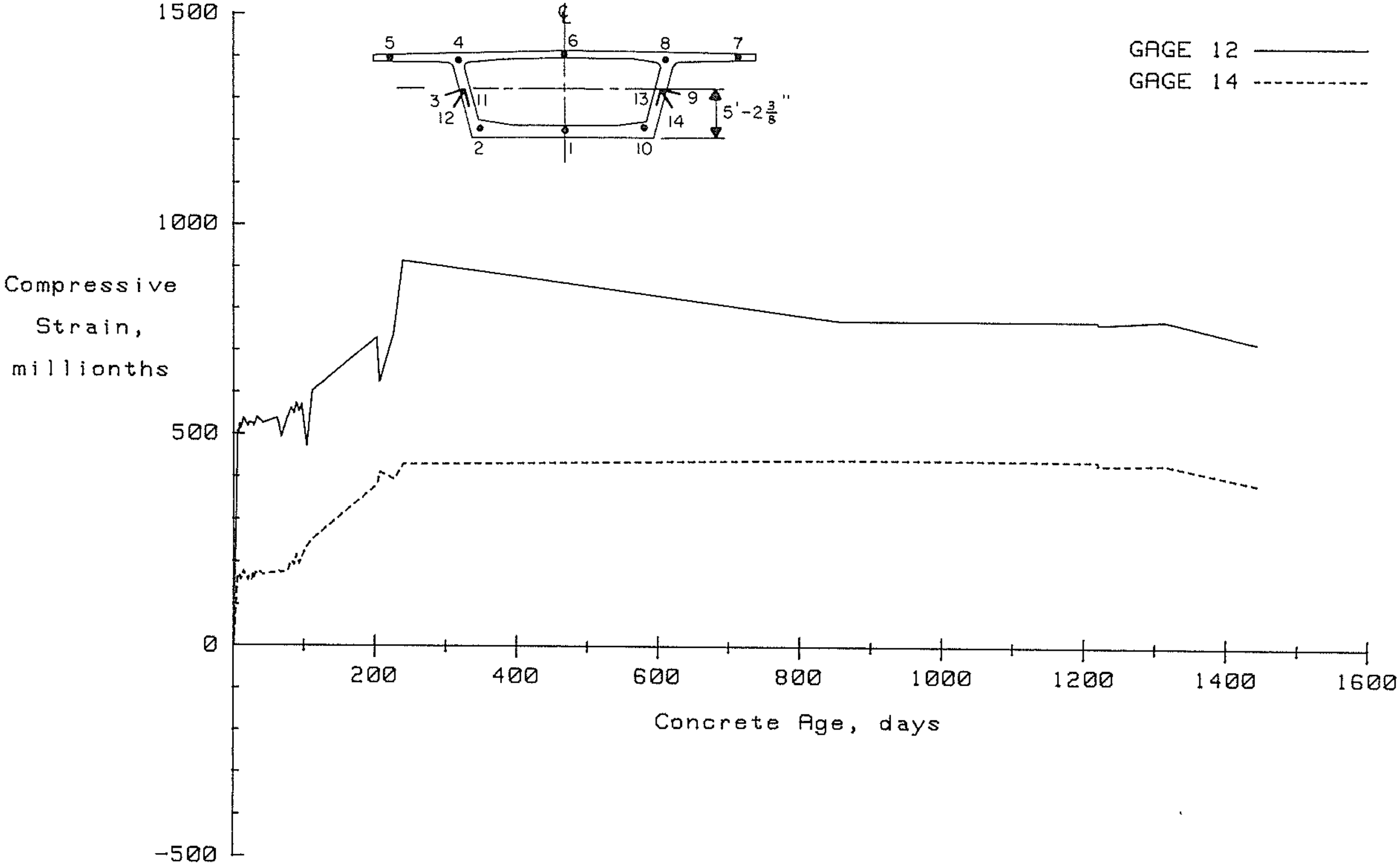

FIG. 5-12 CARLSON STRAIN DATA FOR GAGES 12 AND 14 OF SEGMENT 1313

Figure 37. Carlson strain data for Gages 12 and 14 of Segment 1313.

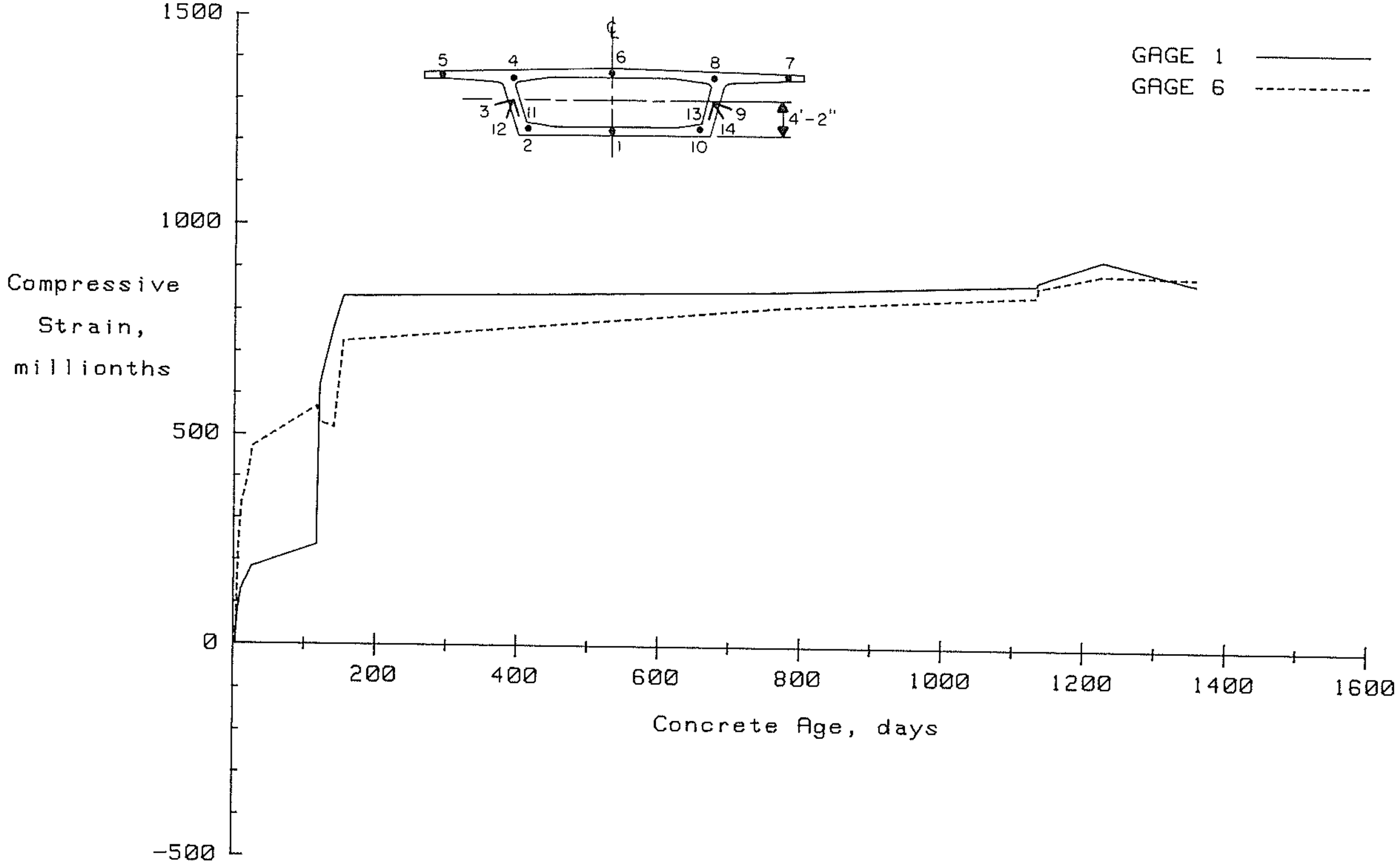

FIG. 5-13 CARLSON STRAIN DATA FOR GAGES 1 AND 6 OF SEGMENT 1323

Figure 38. Carlson strain data for Gages 1 and 6 of Segment 1323.

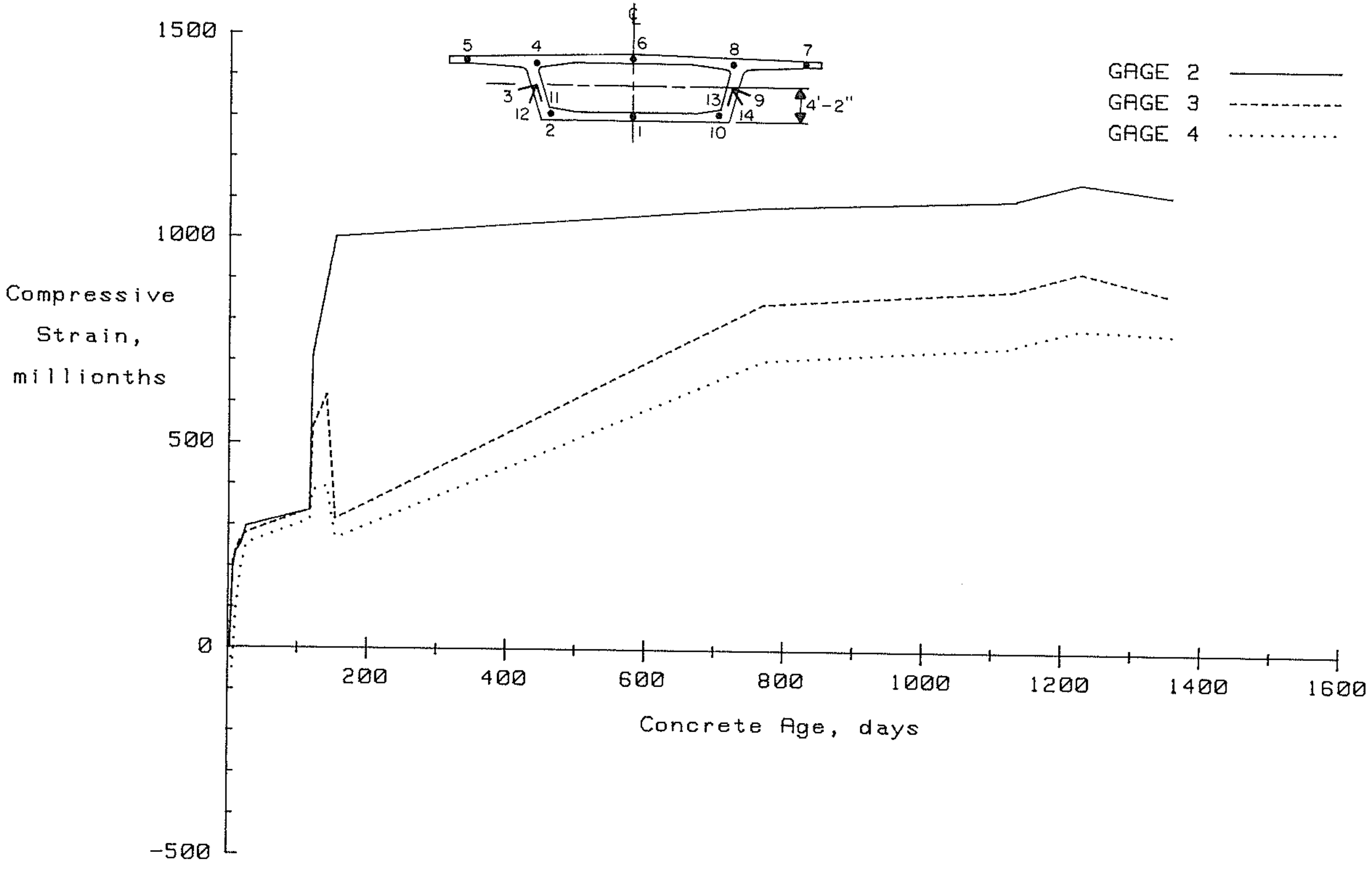

FIG. 5-14 CARLSON STRAIN DATA FOR GAGES 2, 3, AND 4 OF SEGMENT 1323

Figure 39. Carlson strain data for Gages 2, 3, and 4 of Segment 1323.

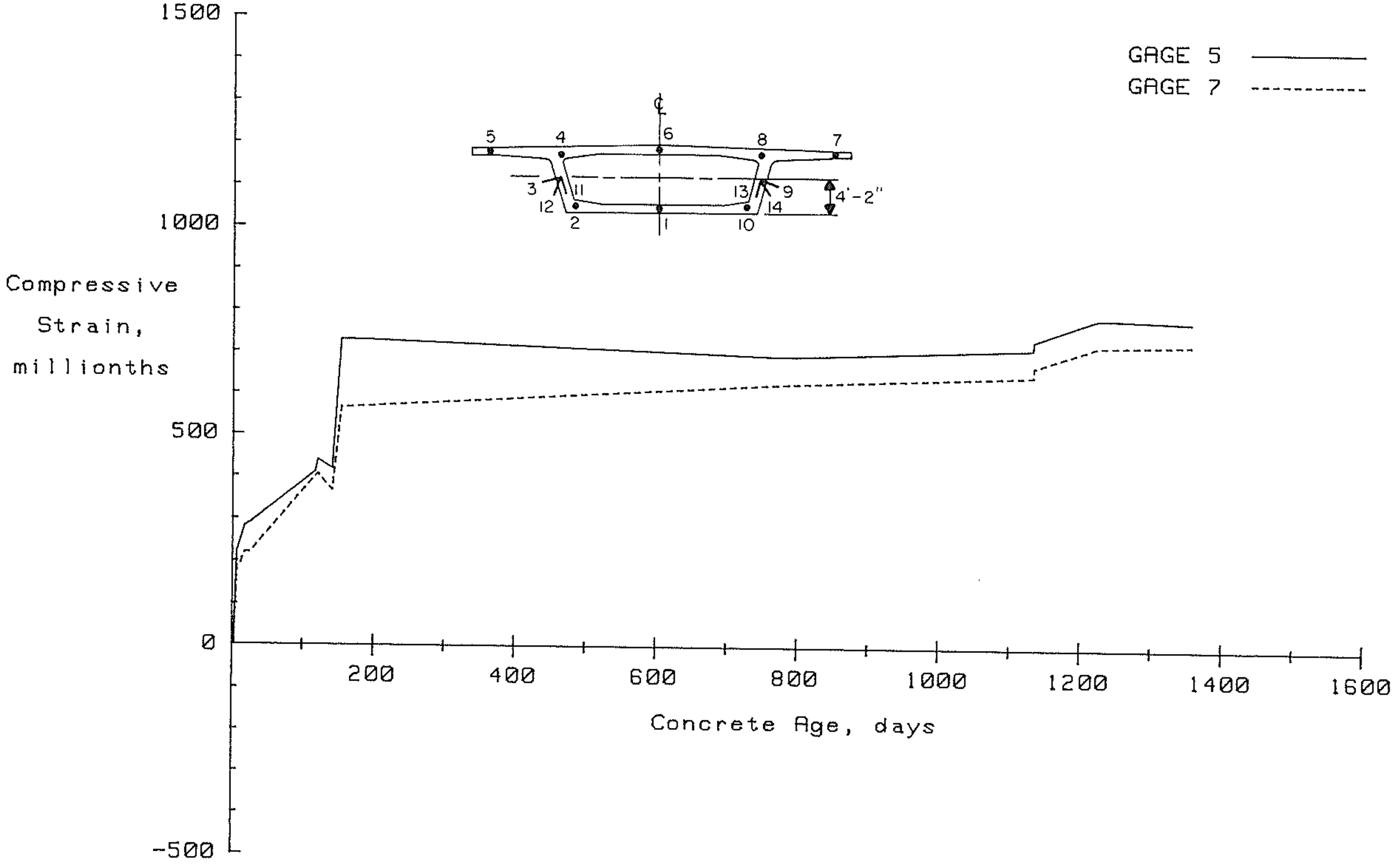

FIG. 5-15 CARLSON STRAIN DATA FOR GAGES 5 AND 7 OF SEGMENT 1323

Figure 40. Carlson strain data for Gages 5 and 7 of Segment 1323.

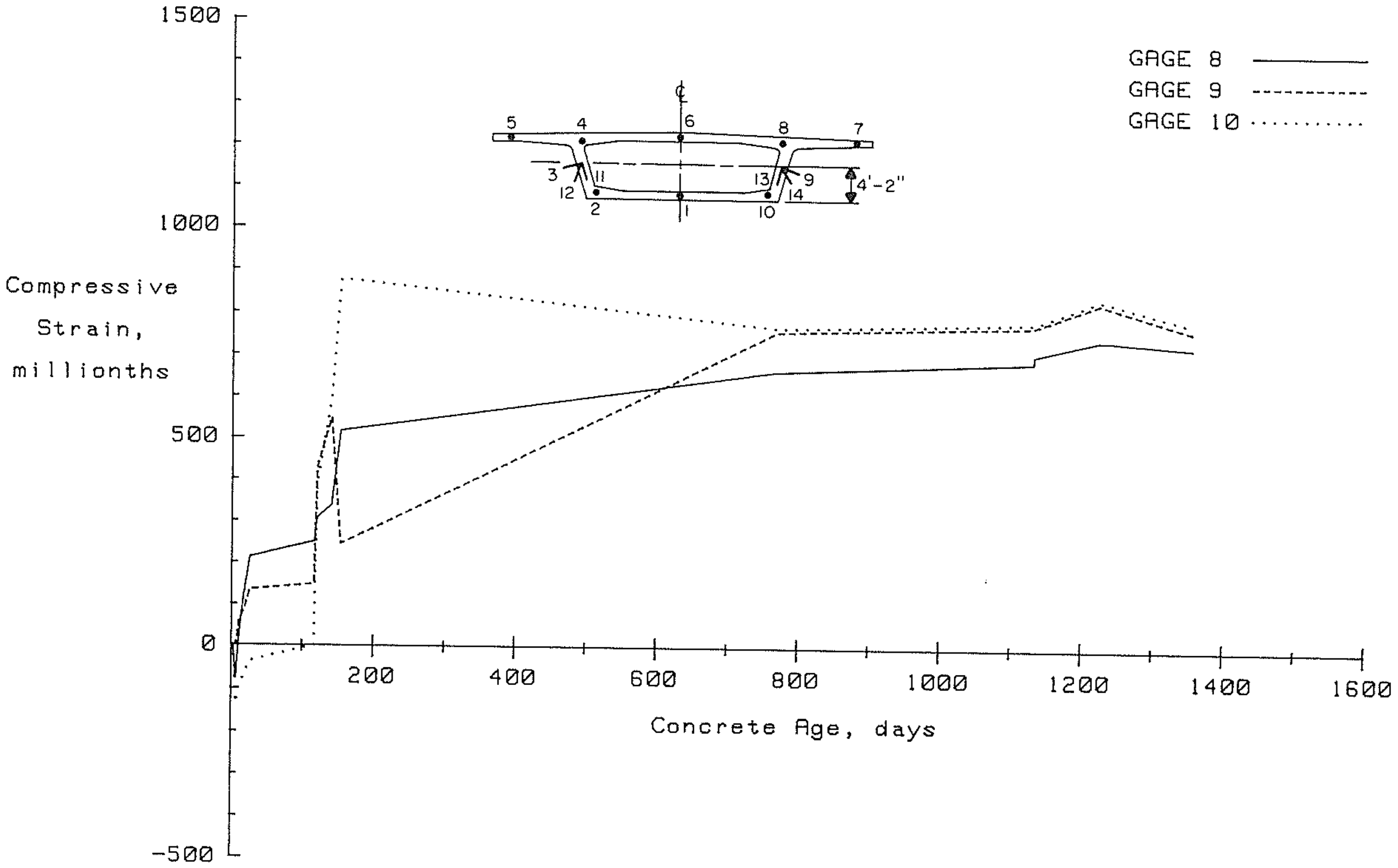

FIG. 5-16 CARLSON STRAIN DATA FOR GAGES 8, 9, AND 10 OF SEGMENT 1323

Figure 41. Carlson strain data for Gages 8, 9, and 10 of Segment 1323.

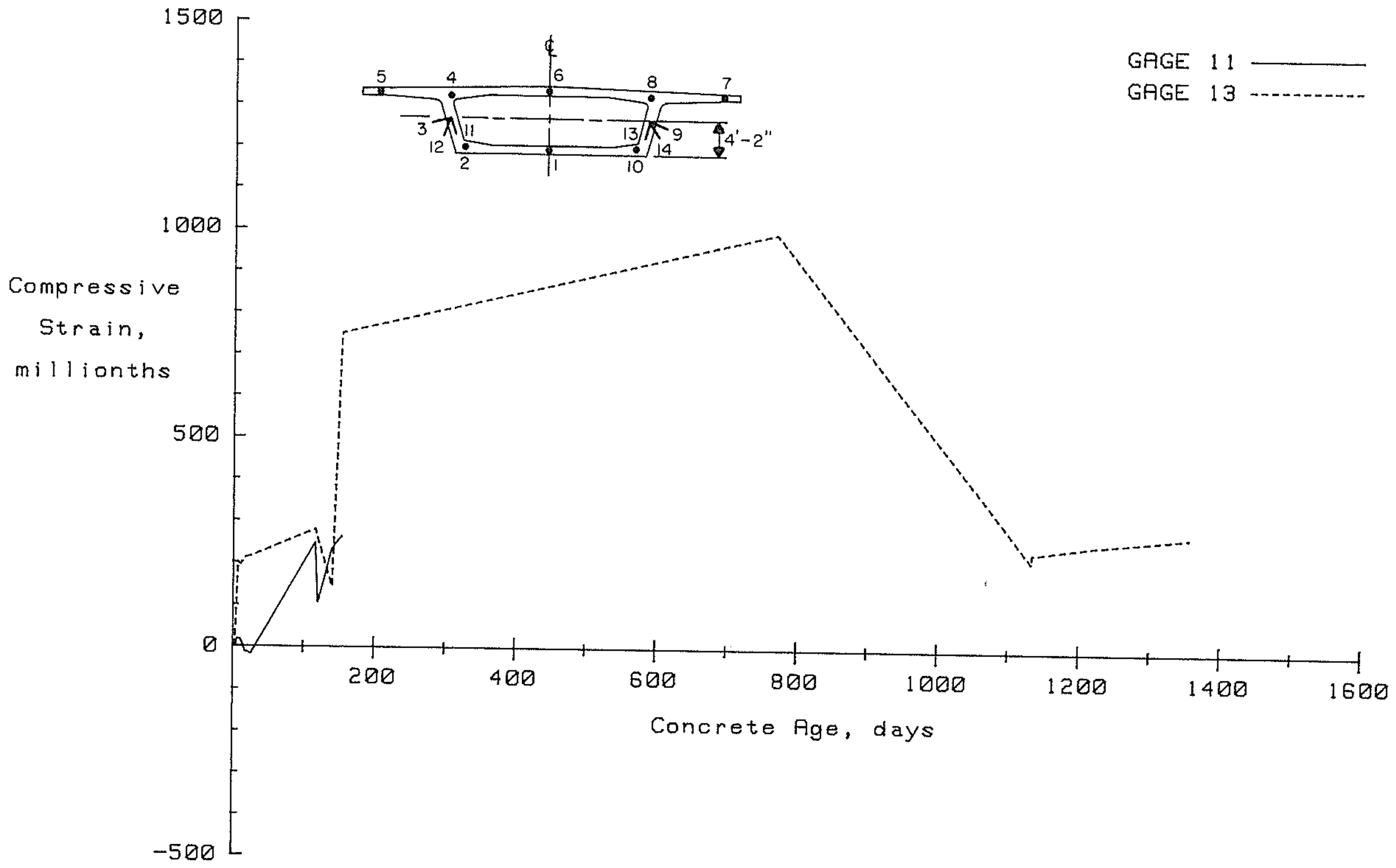

FIG. 5-17 CARLSON STRAIN DATA FOR GAGES 11 AND 13 OF SEGMENT 1323

Figure 42. Carlson strain data for Gages 11 and 13 of Segment 1323.

Figure 21. Access to the inside of the box girder.

Figure 22. Schematic drawing of digital data acquisition system.

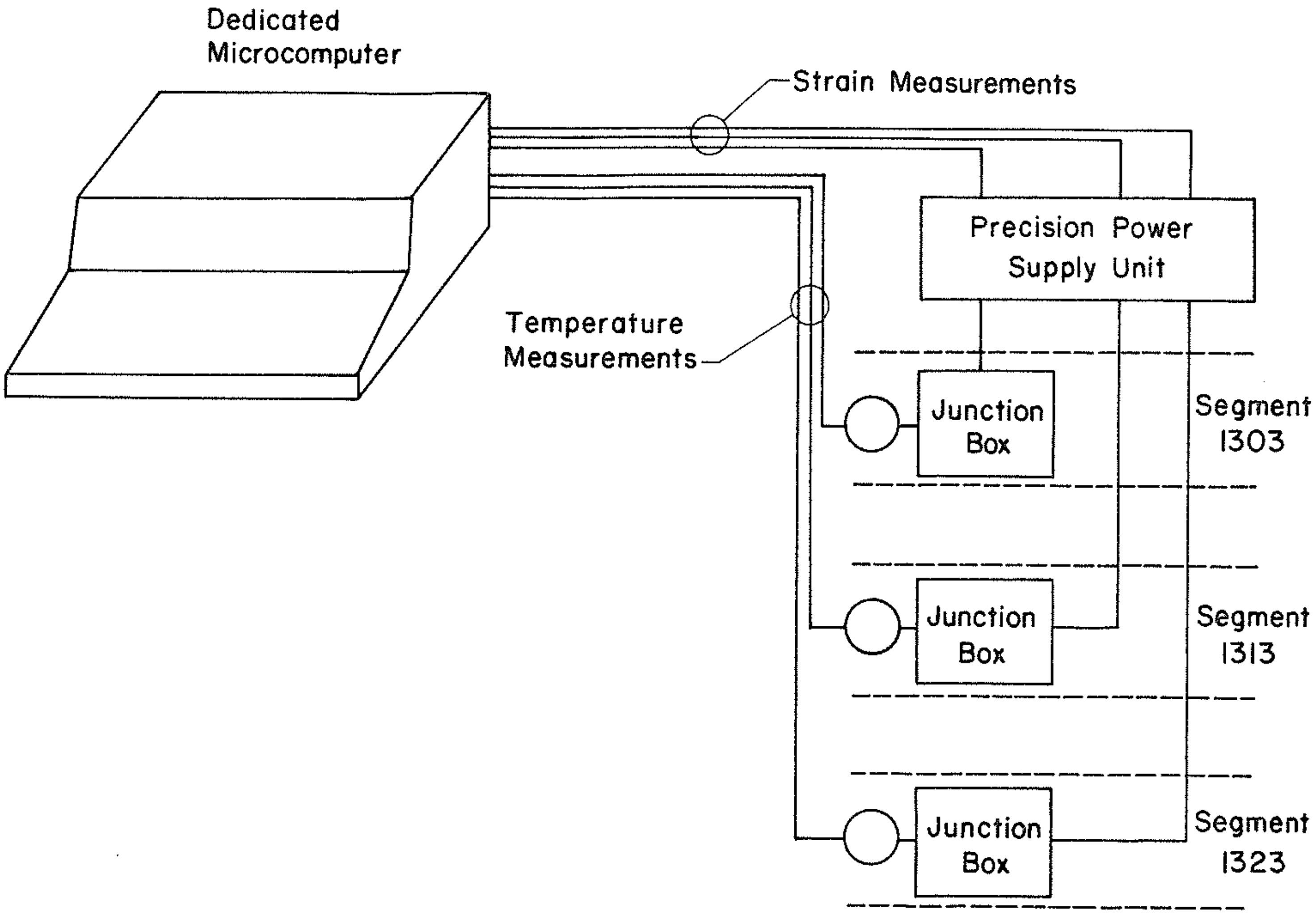

FIG. 4-16 SCHEMATIC DRAWING OF DIGITAL DATA ACQUISITION SYSTEM

Figure 23. Digital data acquisition system.

Figure 24. Control programs.

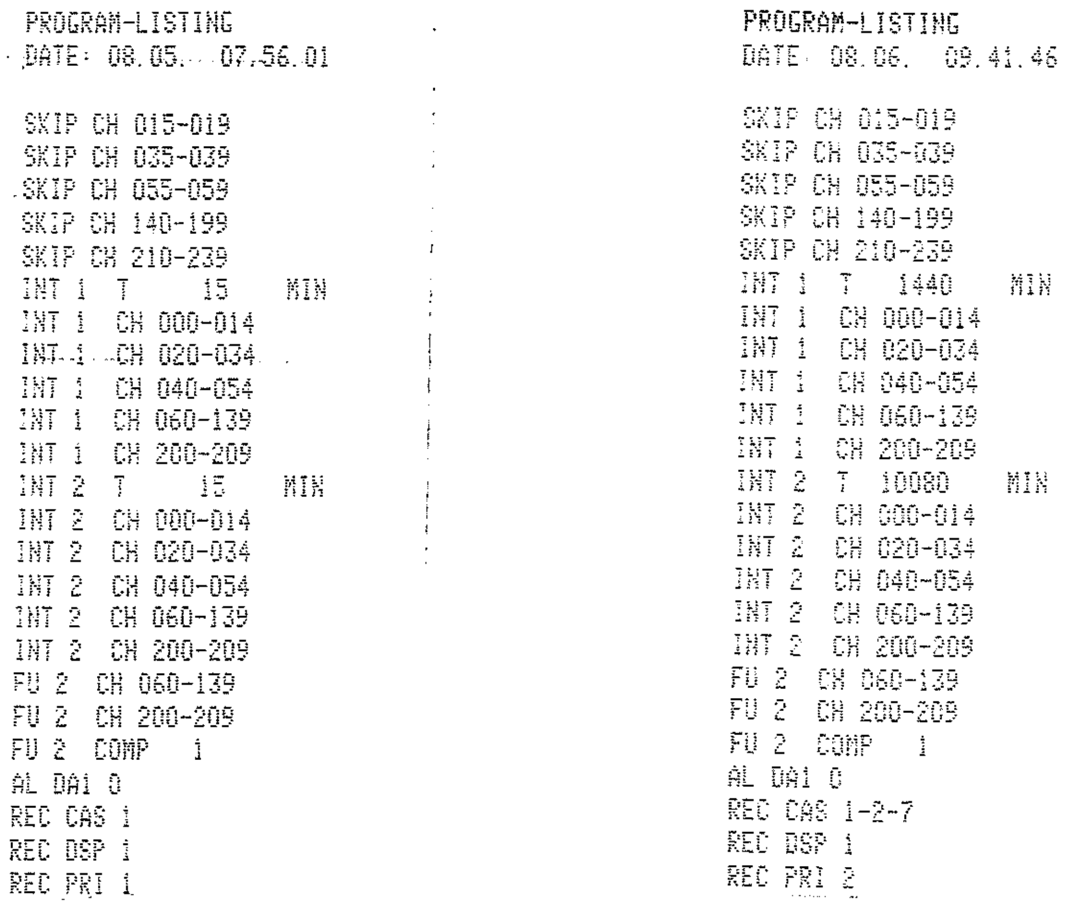

```
PROGRAM-LISTING
DATE: 08.05.   07.56.01

SKIP CH 015-019
SKIP CH 035-039
SKIP CH 055-059
SKIP CH 140-199
SKIP CH 210-239
INT 1  T      15    MIN
INT 1  CH 000-014
INT 1  CH 020-034
INT 1  CH 040-054
INT 1  CH 060-139
INT 1  CH 200-209
INT 2  T      15    MIN
INT 2  CH 000-014
INT 2  CH 020-034
INT 2  CH 040-054
INT 2  CH 060-139
INT 2  CH 200-209
FU 2  CH 060-139
FU 2  CH 200-209
FU 2  COMP   1
AL DA1 0
REC CAS 1
REC DSP 1
REC PRI 1
```

a) 15-MINUTE INTERVAL SCANNING

```
PROGRAM-LISTING
DATE  08.06.   09.41.46

SKIP CH 015-019
SKIP CH 035-039
SKIP CH 055-059
SKIP CH 140-199
SKIP CH 210-239
INT 1  T   1440    MIN
INT 1  CH 000-014
INT 1  CH 020-034
INT 1  CH 040-054
INT 1  CH 060-139
INT 1  CH 200-209
INT 2  T  10080    MIN
INT 2  CH 000-014
INT 2  CH 020-034
INT 2  CH 040-054
INT 2  CH 060-139
INT 2  CH 200-209
FU 2  CH 060-139
FU 2  CH 200-209
FU 2  COMP   1
AL DA1 0
REC CAS 1-2-7
REC DSP 1
REC PRI 2
```

b) DAILY AND WEEKLY INTERVAL SCANNING

FIG. 4-18 CONTROL PROGRAMS

Figure 25. Recorded data printout.

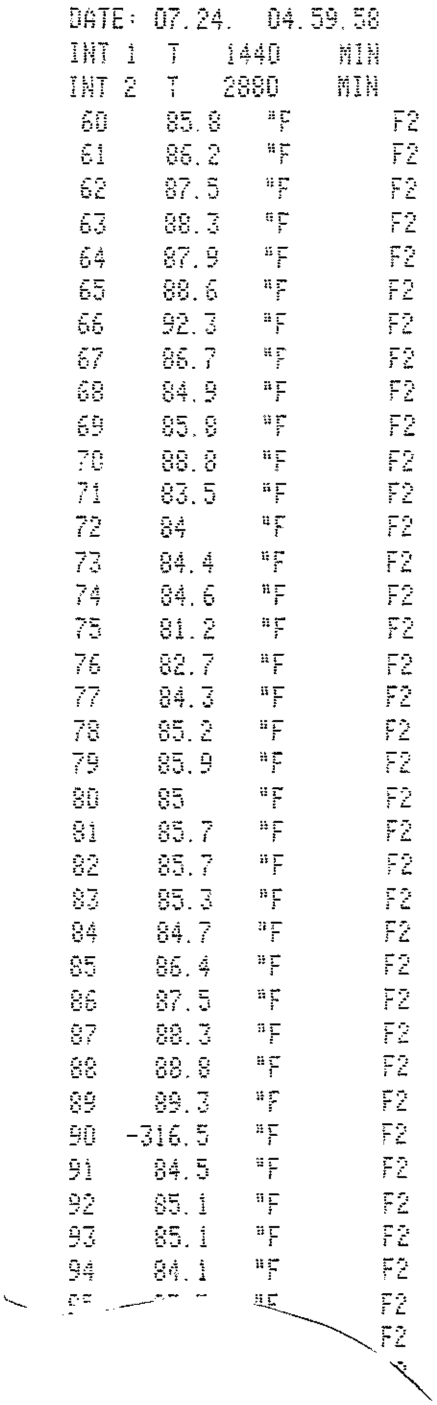

```
DATE: 07.24.  04.59.58
INT 1  T   1440    MIN
INT 2  T   2880    MIN
 60    85.8   °F        F2
 61    86.2   °F        F2
 62    87.5   °F        F2
 63    88.3   °F        F2
 64    87.9   °F        F2
 65    88.6   °F        F2
 66    92.3   °F        F2
 67    86.7   °F        F2
 68    84.9   °F        F2
 69    85.8   °F        F2
 70    88.8   °F        F2
 71    83.5   °F        F2
 72    84     °F        F2
 73    84.4   °F        F2
 74    84.6   °F        F2
 75    81.2   °F        F2
 76    82.7   °F        F2
 77    84.3   °F        F2
 78    85.2   °F        F2
 79    85.9   °F        F2
 80    85     °F        F2
 81    85.7   °F        F2
 82    85.7   °F        F2
 83    85.3   °F        F2
 84    84.7   °F        F2
 85    86.4   °F        F2
 86    87.5   °F        F2
 87    88.3   °F        F2
 88    88.8   °F        F2
 89    89.3   °F        F2
 90  -316.5   °F        F2
 91    84.5   °F        F2
 92    85.1   °F        F2
 93    85.1   °F        F2
 94    84.1   °F        F2
                        F2
                        F2
```

FIG. 4-19 RECORDED DATA PRINTOUT

FIELD-MEASURED DATA

Measured field data are presented in this section. A schedule of collected data with the corresponding construction event for the three instrumented segments is given in Table 2. With the exception of the first two readings of each gage, LTRC personnel took all measurements. CTL took the first two readings for each gage. Data are presented under the following categories: concrete strain measurements, temperature measurements, deflection measurements, rotation measurements, 24-hour measurements, and shear strain measurements.

CONCRETE STRAIN MEASUREMENTS

Collected Carlson strain readings were sent to CTL by LTRC for data reduction. Strain readings were reduced with a microcomputer. Reduced concrete strains and concrete temperatures for each installed Carlson strain meter are tabulated in another report (12).

Measured concrete strains represent concrete movements recorded between the date of the measurement and the zero readings taken before concrete casting. Strain readings listed in this report have been temperature adjusted to the reference temperature of 73°F. Temperature adjustments were made so that readings can be compared. The linear coefficient of thermal expansion for concrete was assumed to be 5.5-millionths/°F. Coefficients of thermal expansion for Carlson strain meters were based on the data supplied by the meter manufacturer. Temperature-induced movements were assumed to be totally unrestrained.

Relationships of measured concrete compressive strains since the zero readings versus ages of concrete for Segments 1303, 1313, and 1323 are shown in Figures 26 through 31, 32 through 37, and 38 through 43, respectively. It is noted that the first two readings were not plotted in the figures because of the heavy influence of the heat of hydration in the strain readings. The horizontal axis in the figures represents the number of days since concrete casting of the bridge segment, or simply the concrete age of the segment. The vertical axis represents the concrete shortening per unit length at the measured location.

TABLE 2
READING SCHEDULE

Date	Events	Concrete Age, Days		
		Segment 1303	Segment 1313	Segment 1323
9/17/83	One Day After Casting of Segment 1303	1		
9/23/83	Removal of Formwork and Post Tensioning	7		
10/03/83	Casting of Segment 1304	17		
10/05/83	Stressing of Segment 1304	19		
10/07/83	Casting of Segment 1305	21		
10/10/83	Stressing of Segment 1305	24		
10/13/83	Casting of Segment 1306	27		
10/14/83	Stressing of Segment 1306	28		
10/17/83	Casting of Segment 1307	31		
10/19/83	Stressing of Segment 1307	33		
10/02/83	Casting of Segment 1308	35		
10/24/83	Stressing of Segment 1308	38		
10/26/83	Casting of Segment 1309	40		
10/28/83	Casting of Segment 1310	42		
10/31/83	Stressing of Segment 1310	45		
11/03/83	Casting of Segment 1311	48		
11/04/83	Casting of Segment 1312	49		
11/07/83	Before Stressing of Segment 1312	52		
11/07/83	After Stressing of Segment 1312	52		
11/10/83	One Day After Casting of Segment 1313	55	1	
11/15/83	Stressing of Segment 1313	60	6	
11/17/83	Before Stressing of Segment 1314	62	8	
11/18/83	After Stressing of Segment 1314	63	9	
11/20/83	Casting of Segment 1315	65	11	
11/23/83	Stressing of Segment 1315	68	14	
11/30/83	Casting of Segment 1316	75	21	
12/01/83	Stressing of Segment 1316	76	22	
12/05/83	Casting of Segment 1317	80	26	
12/07/83	Stressing of Segment 1317	82	28	
12/08/83	Casting of Segment 1318	83	29	
12/13/83	Casting of Segment 1319	88	34	
12/21/83	Stressing of Segment 1319	95	42	
1/09/84	Casting of Segment 1320	114	61	
1/11/84	Stressing of Segment 1320	116	63	
1/16/84	Casting of Segment 1321	121	68	
1/25/84	Casting of Segment 1322	130	77	
1/30/84	Stressing of Segment 1322, cable slipped and replaced	135	82	
2/03/84	Stressing of Segment 1322	139	86	
2/06/84	Three Days After Casting of Segment 1323	142	89	3

TABLE 2
READING SCHEDULE (Continued)

Date	Events	Concrete Age, Days		
		Segment 1303	Segment 1313	Segment 1323
2/10/84	Stressing of Segment 1323	146	94	7
2/14/84	Casting of Segment 1324	150	97	11
2/21/84	Stressing of Segment 1324	157	104	18
3/02/84	Casting of Segment 1325	166	112	26
6/01/84	Casting of Closure Segment for Piers 12 & 13	257	203	117
6/05/84	Post-Tensioning of Closure Segment	261	207	121
6/25/84	Final Post-Tensioning of the Instrumented Span	281	227	141
10/17/84	Installation of Guard Rail and Roadway Overlay	395	240	154
6/26/86	Routine Readings	1012	857	771
6/23/87	Trouble-Shooting of Data Acquisition System	1375	1220	1134
6/24/87	24-hour Readings in Summer	1376	1221	1135
9/23/87	24-hour Readings in Fall	1467	1312	1226
2/01/87	24-hour Readings in Winter	1596	1443	1357

TEMPERATURE MEASUREMENTS

Whenever Carlson strain readings were taken, temperature readings from installed thermocouples were taken also. Recorded concrete temperatures versus ages of concrete for instrumented Segments 1303, 1313, and 1323 are shown in Figures 44 through 48, 49 through 53, and 54 through 58, respectively. The horizontal axis of these figures represents the number of days since concrete casting of the bridge segments. The vertical axis represents measured temperature in degrees Fahrenheit. Gage number and corresponding locations in the bridge segment are also illustrated in the figures.

As shown in Figures 44, 49, and 54, maximum temperature differentials between thermocouples at the top and bottom slabs are approximately 20°F. Temperature differential across the depth of a slab, however, was on the order of 10°F.

DEFLECTION MEASUREMENTS

The second deflection measuring scheme was established on June 28, 1984. Subsequent deflection profiles of six bridge segments were taken by LTRC. The six bridge segments were Segments 1303, 1304, 1313, 1314, 1323, and 1324. The first deflection readings taken on April 3, 1985 indicated that deflection points at Segment 1313, (east and west), Segment 1304, (east) and Segment 1314 (east) were destroyed during construction. Consequently, new deflection points at those four locations were reset on April 3, 1985.

In Table 2, both recorded elevation readings and relative deflections at the measurement locations are listed. Elevation readings represent the actual elevations of the deflection points using the bench mark No. 6 with its elevation at 145.394 ft. Elevation profiles of the east deflection points on June 28, 1984, and April 3, 1985, are shown in Figure 59. The profiles represent the actual deflected shape of the Red River Bridge after completion of construction. As indicated in Table 3, deflection measuring points were reset for Segment 1313 (east and west), Segment 1304 (east), and Segment 1314 (east). Effects of the resetting of deflection points are shown in Figure 59 as the unevenness in the elevation profiles.

TABLE 3
DEFLECTION MEASUREMENTS

Segment	Location	Elevation Readings (Relative Deflection). ft							
		6/28/84	4/3/85	8/8/85	7/10/86	11/7/86	9/24/87	2/1/88	5/9/88
1323	East	155.47 (0.00)	155.26 (0.21)	155.28 (0.19)	155.23 (0.24)	155.25 (0.22)	155.25 (0.22)	155.18 (0.29)	155.19 (0.28)
	West	155.46 (0.00)	155.23 (0.23)	155.27 (0.19)	155.23 (0.23)	155.26 (0.20)	155.24 (0.22)	155.19 (0.27)	155.20 (0.26)
1313	East	154.52 (destroyed)	154.77 (0.00)	154.78 (-0.01)	154.75 (0.03)	154.77 (-0.00)	154.81 (-0.04)	154.73 (0.04)	154.75 (0.02)
	West	154.51 (destroyed)	154.81 (0.00)	154.82 (-0.01)	154.78 (0.03)	154.81 (-0.00)	154.78 (-0.03)	154.77 (0.04)	154.79 (0.02)
1303	East	153.33 (0.00)	153.29 (0.04)	153.31 (0.02)	153.29 (0.04)	153.31 (0.02)	153.33 (0.00)	153.30 (0.03)	153.31 (0.02)
	West	153.36 (0.00)	153.32 (0.04)	153.33 (0.03)	153.31 (0.05)	153.34 (0.02)	153.34 (0.02)	153.33 (0.03)	153.34 (0.02)
1304	East	152.45 (destroyed)	152.79 (0.00)	152.80 (-0.01)	152.78 (0.01)	152.83 (-0.04)	152.83 (-0.04)	151.81 (-0.02)	152.82 (-0.03
	West	152.55 (0.00)	152.49 (0.05)	152.49 (0.05)	152.47 (0.07)	152.52 (0.02)	152.51 (0.03)	152.52 (0.02)	152.52 (0.02)
1314	East	150.75 (destroyed)	151.00 (0.00)	151.01 (-0.01)	150.98 (0.02)	151.03 (-0.03)	151.02 (-0.02)	150.99 (0.01)	151.00 (0.00)
	West	150.75 (0.00)	150.68 (0.07)	150.70 (0.05)	150.68 (0.07)	150.71 (0.04)	150.69 (0.06)	150.69 (0.06)	150.69 (0.06)
1324	East	148.66 (0.00)	148.57 (0.09)	148.63 (0.03)	148.56 (0.11)	148.62 (0.05)	148.58 (0.09)	148.57 (0.10)	148.56 (0.11)
	West	148.69 (0.00)	148.61 (0.08)	148.64 (0.05)	148.60 (0.09)	148.61 (0.08)	148.58 (0.11)	148.58 (0.11)	148.59 (0.10)

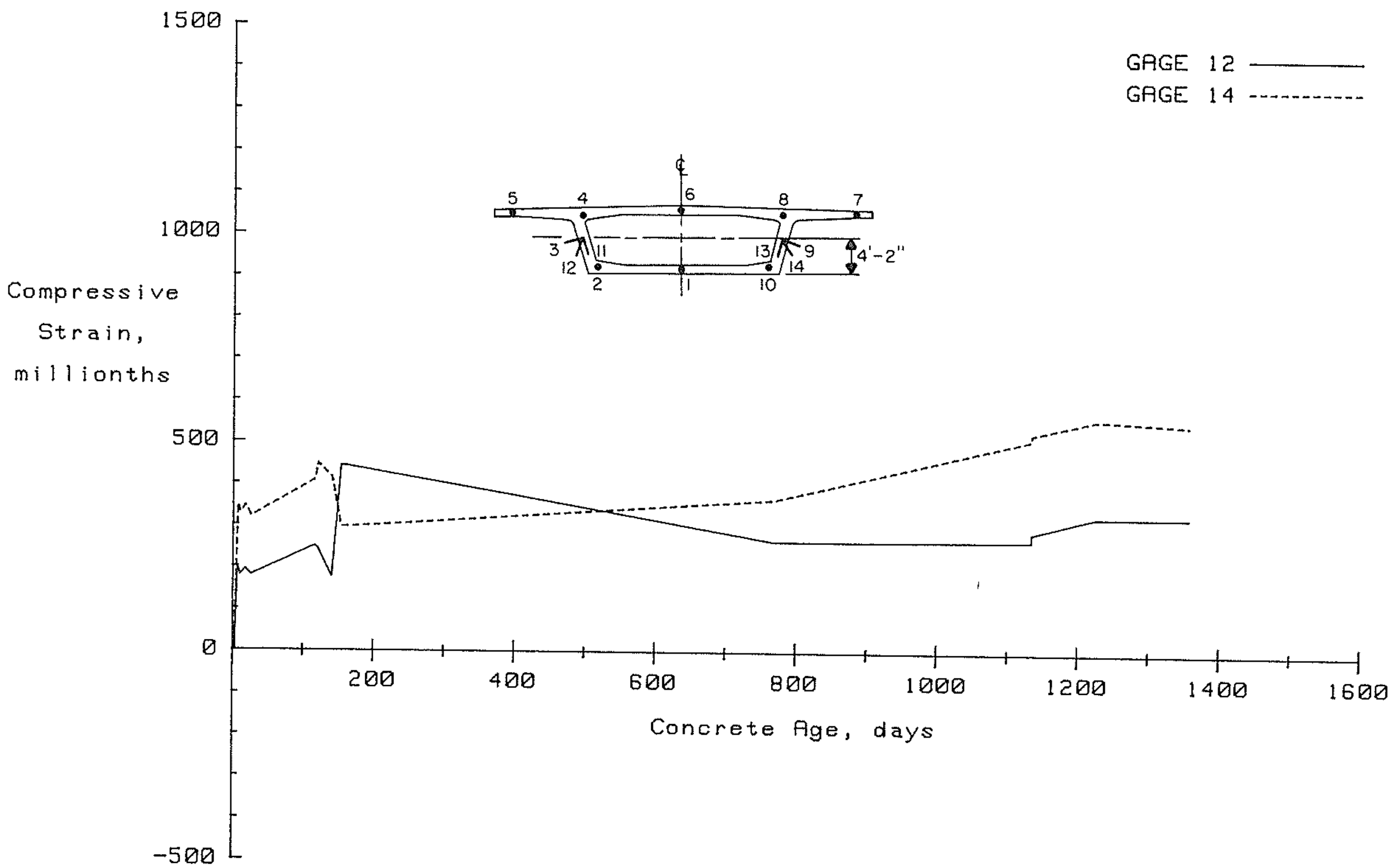

FIG. 5-18 CARLSON STRAIN DATA FOR GAGES 12 AND 14 OF SEGMENT 1323

Figure 43. Carlson strain data for Gages 12 and 14 of Segment 1323.

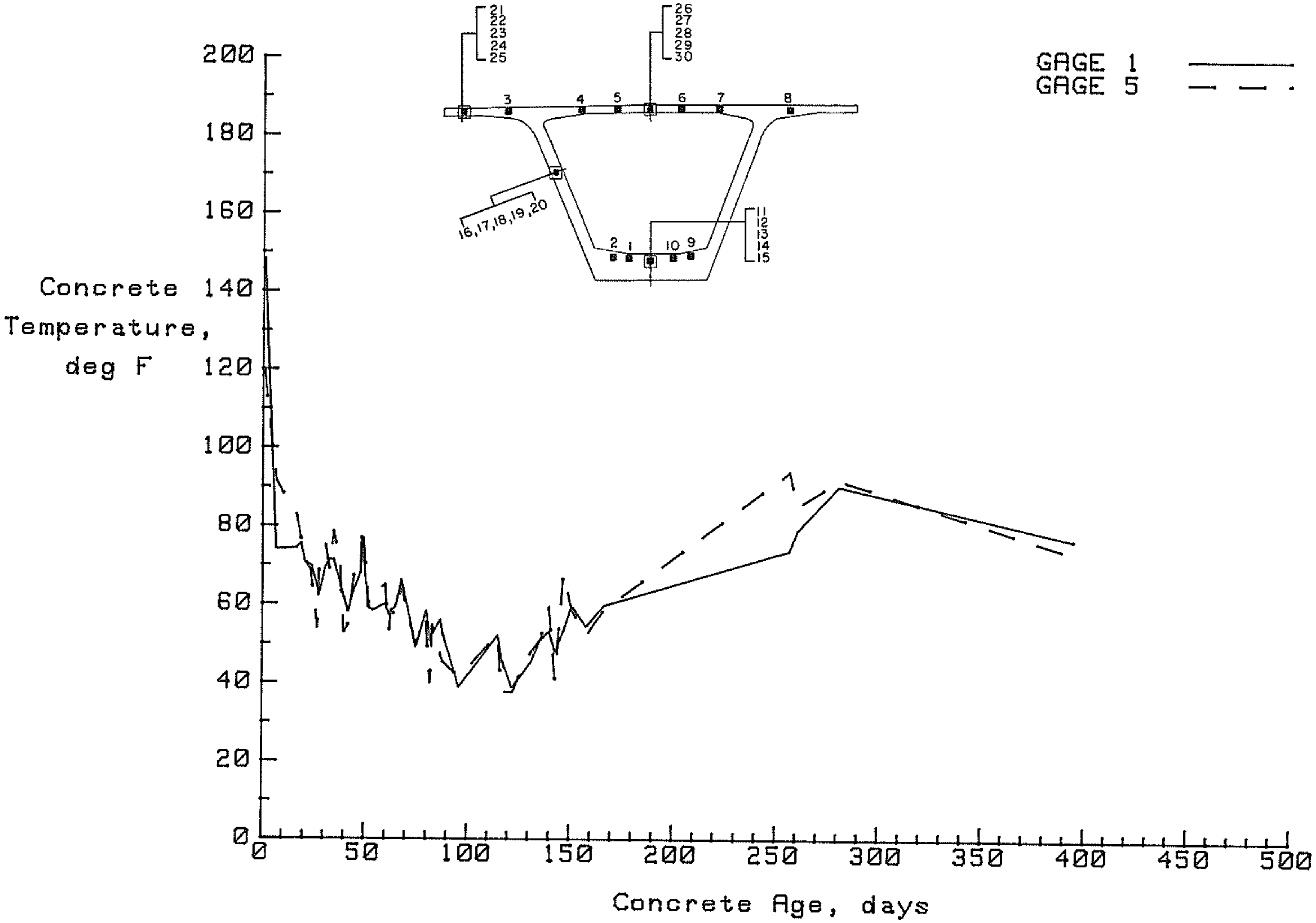

FIG. 5-19 THERMOCOUPLE READINGS FOR GAGES 1 AND 5 OF SEGMENT 1303

Figure 44. Thermocouple readings for Gages 1 and 5 of Segment 1303.

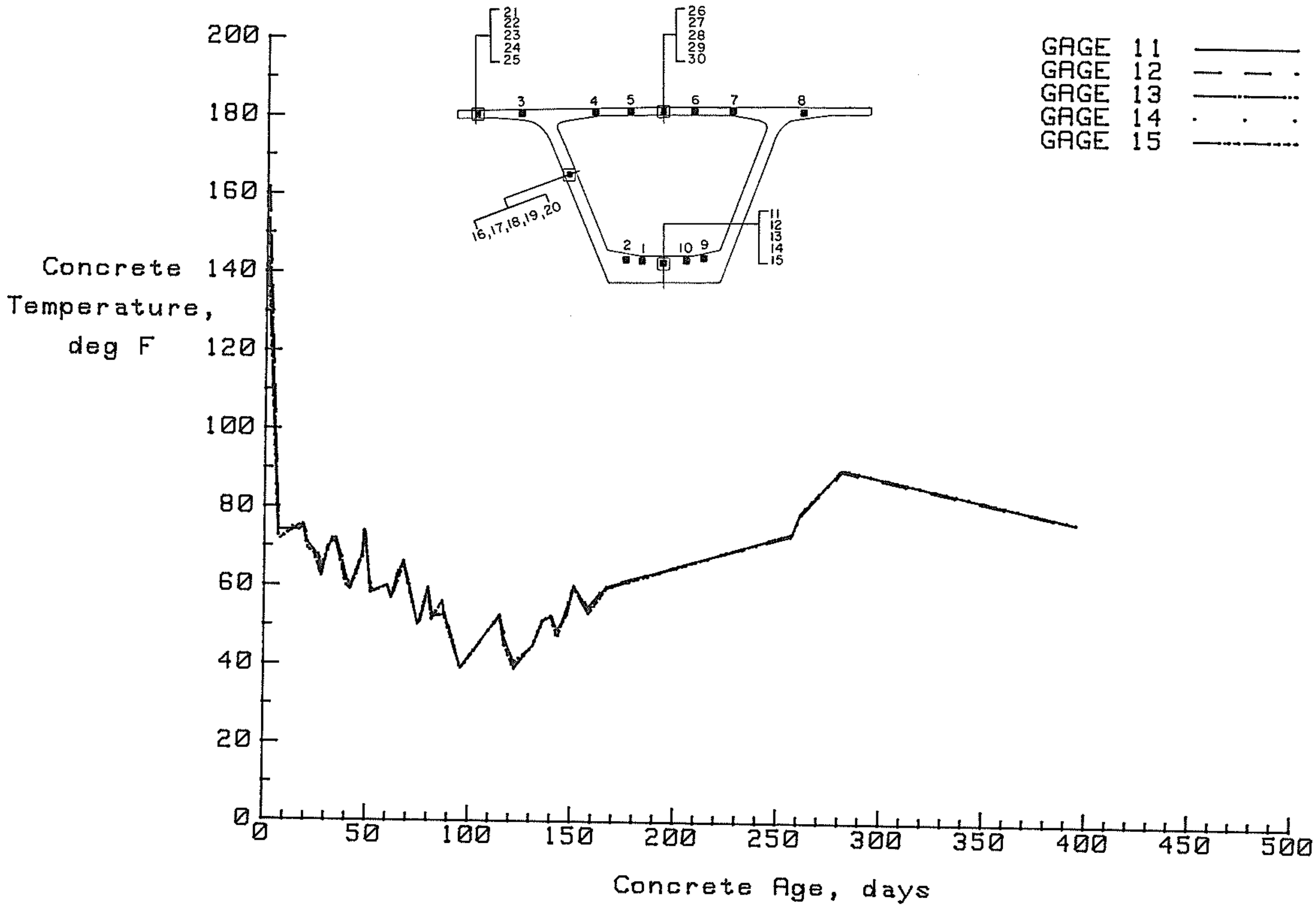

FIG. 5-20 THERMOCOUPLE READINGS FOR GAGES 11, 13, 13, 14, AND 15 OF SEGMENT 1303

Figure 45. Thermocouple readings for Gages 11, 12, 13, 14, and 15 of Segment 1303.

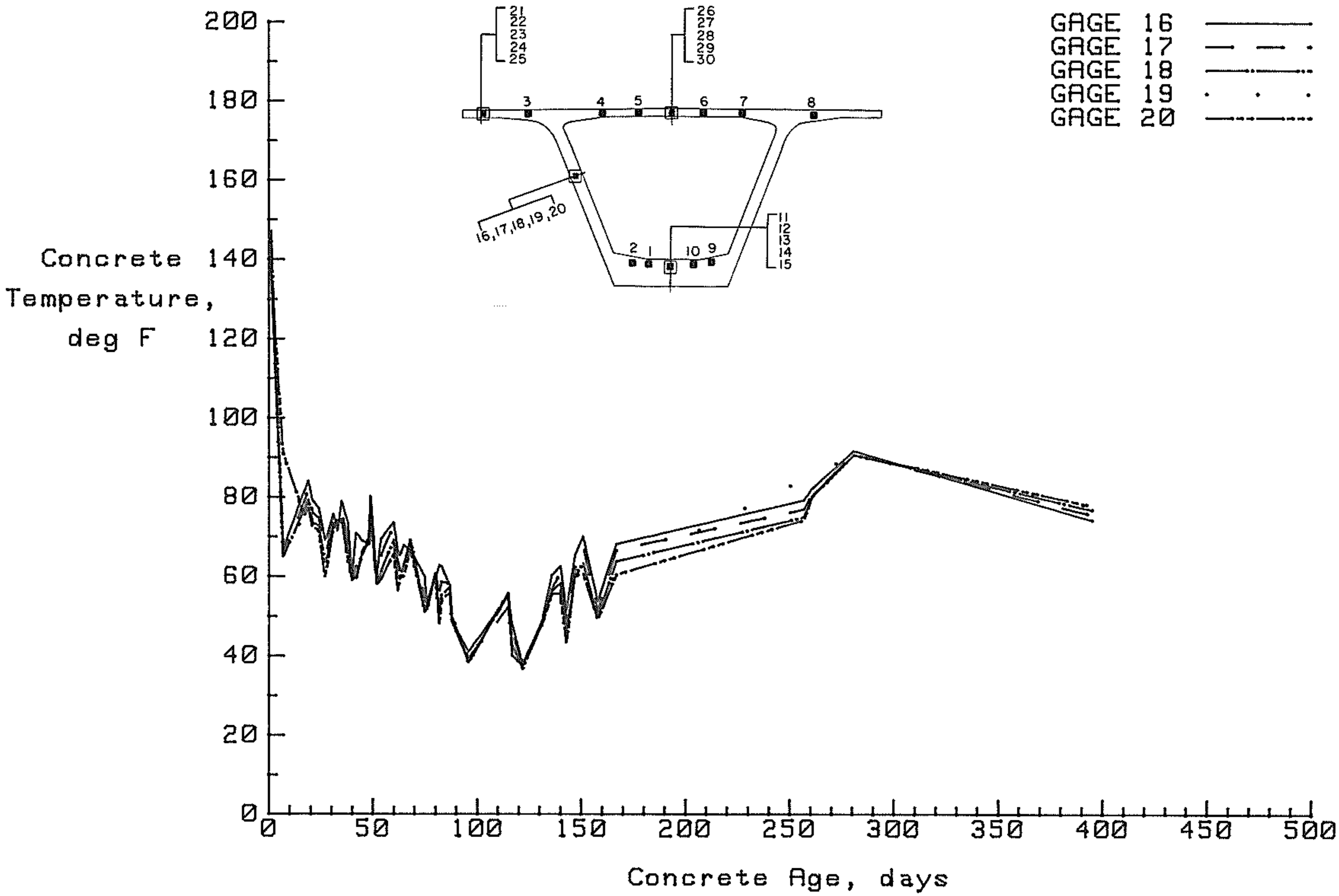

FIG. 5-21 THERMOCOUPLE READINGS FOR GAGES 16, 17, 18, 19, AND 20 OF SEGMENT 1303

Figure 46. Thermocouple readings for Gages 16, 17, 18, 19, and 20 of Segment 1303.

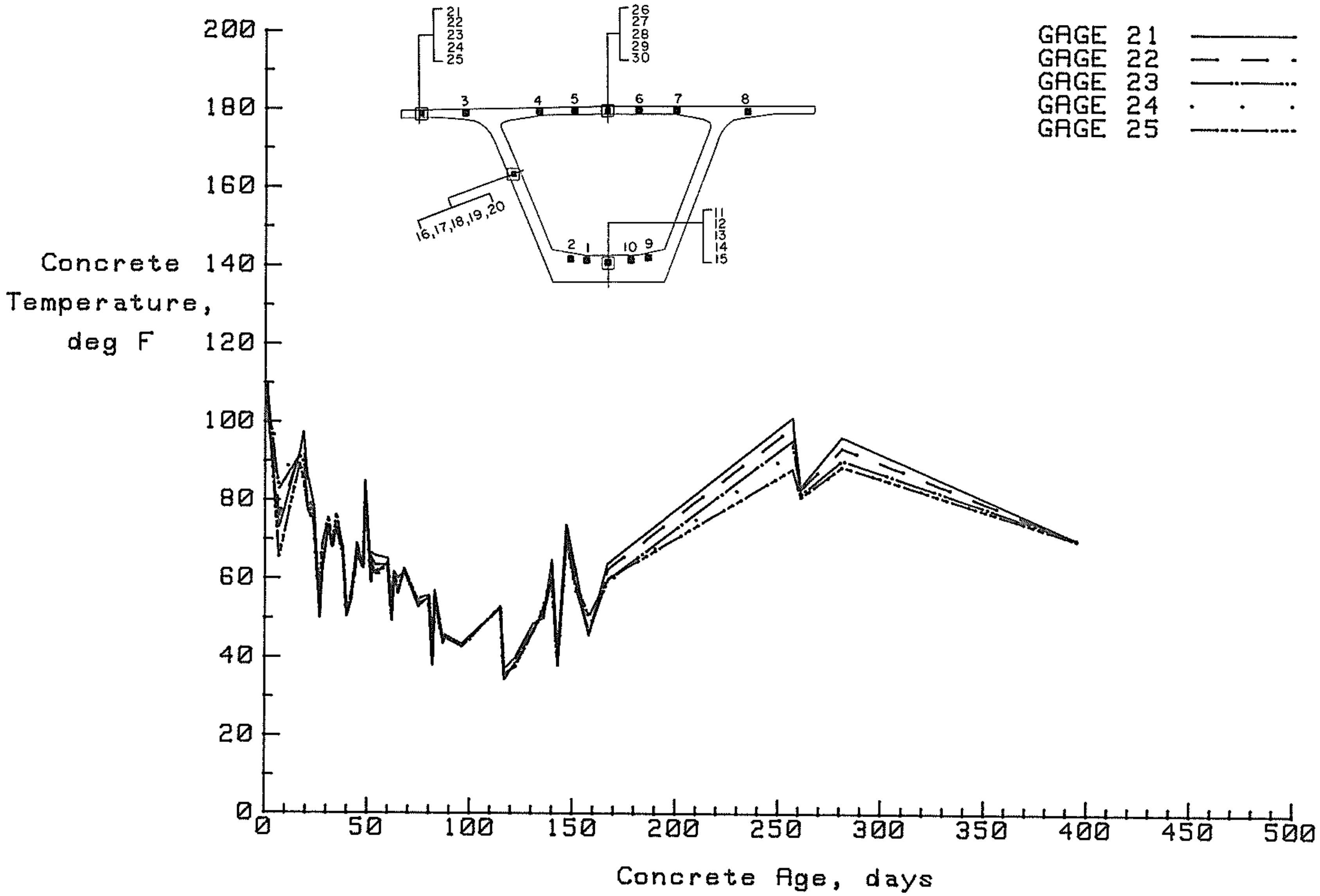

FIG. 5-22 THERMOCOUPLE READINGS FOR GAGES 21, 22, 23, 24, AND 25 OF SEGMENT 1303

Figure 47. Thermocouple readings for Gages 21, 22, 23, 24, and 25 of Segment 1303.

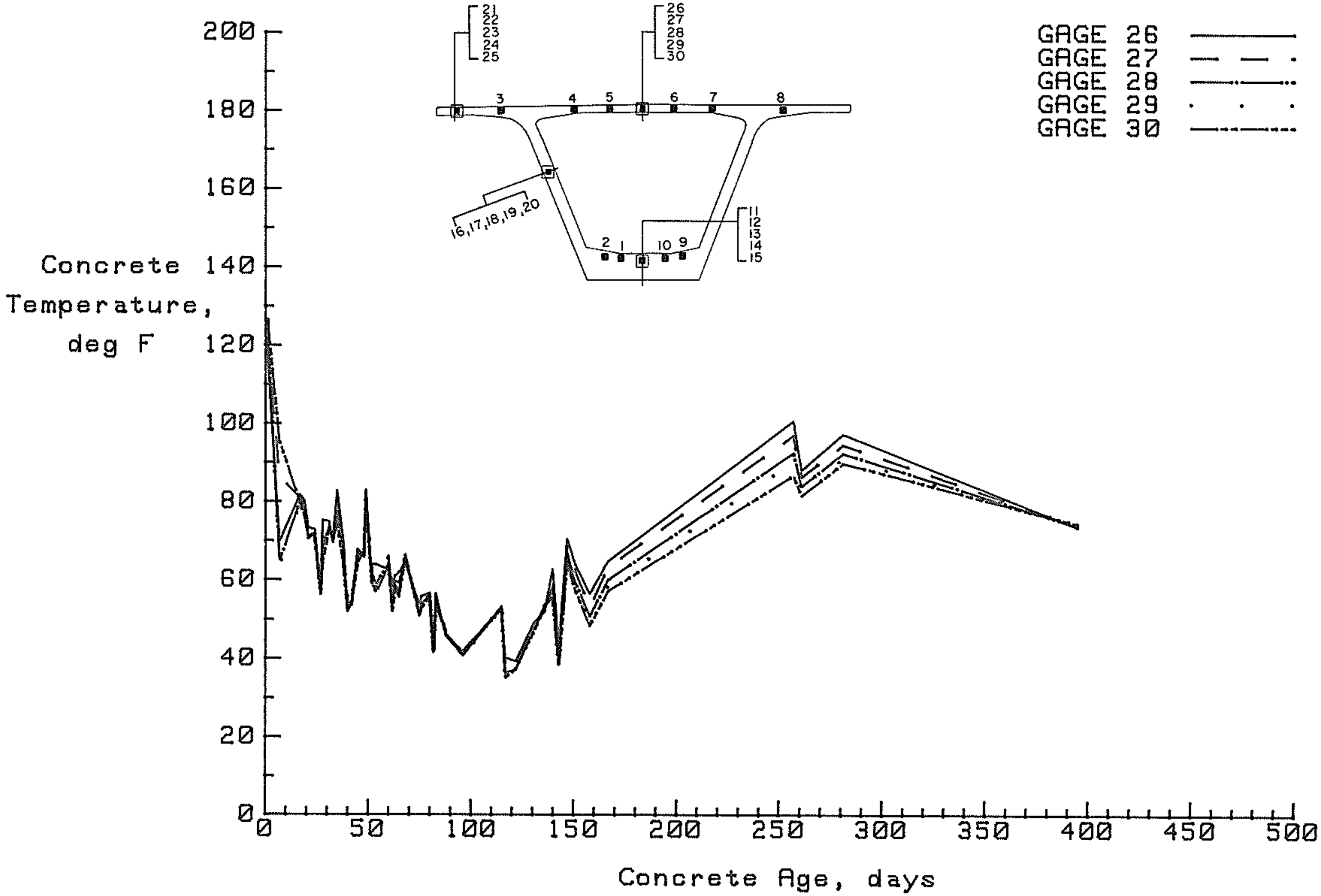

FIG. 5-23 THERMOCOUPLE READINGS FOR GAGES 26, 27, 28, 29, AND 30 OF SEGMENT 1303

Figure 48. Thermocouple readings for Gages 26, 27, 28, 29, and 30 of Segment 1303.

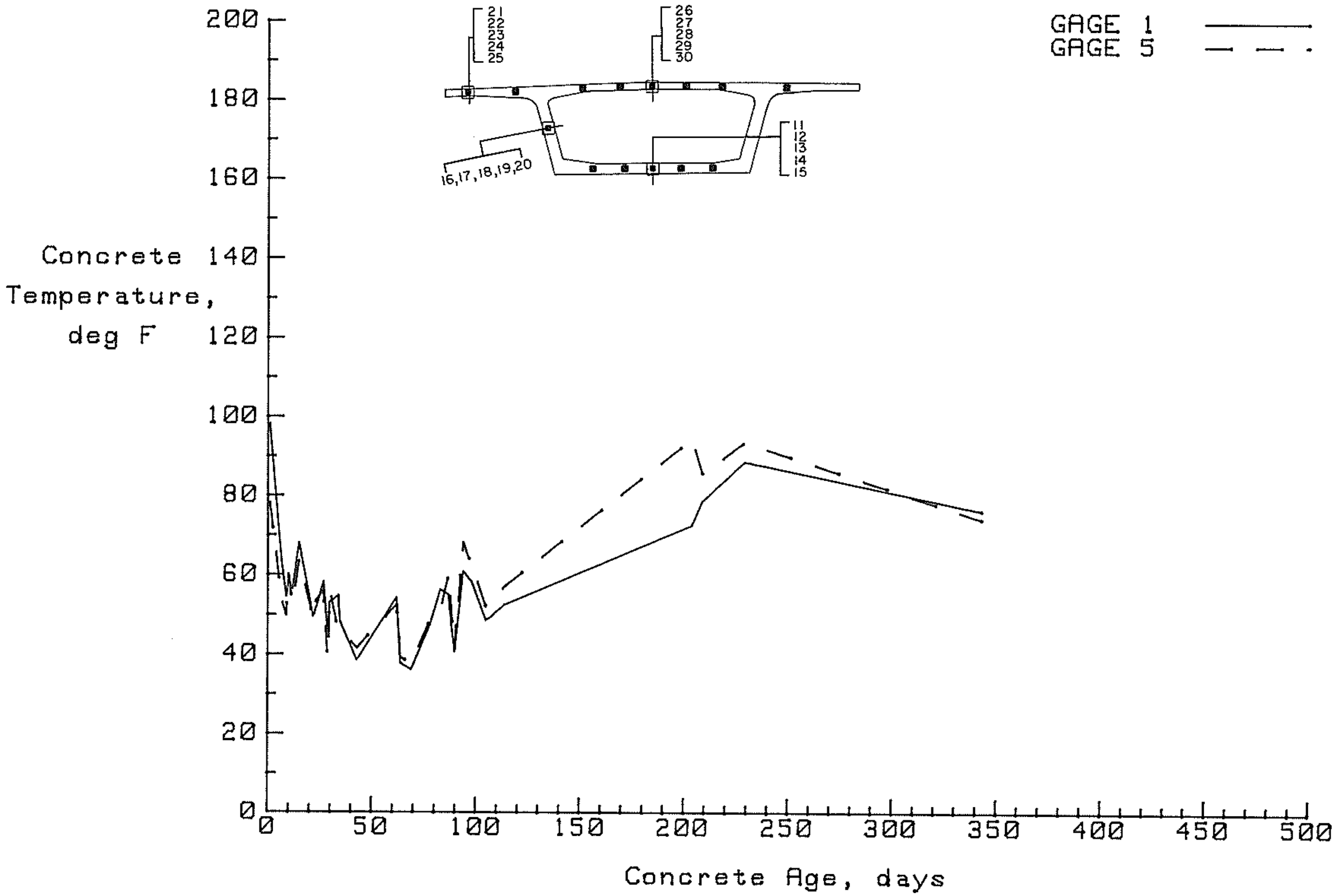

FIG. 5-24 THERMOCOUPLE READINGS FOR GAGES 1 AND 5 OF SEGMENT 1313

Figure 49. Thermocouple readings for Gages 1 and 5 of Segment 1313.

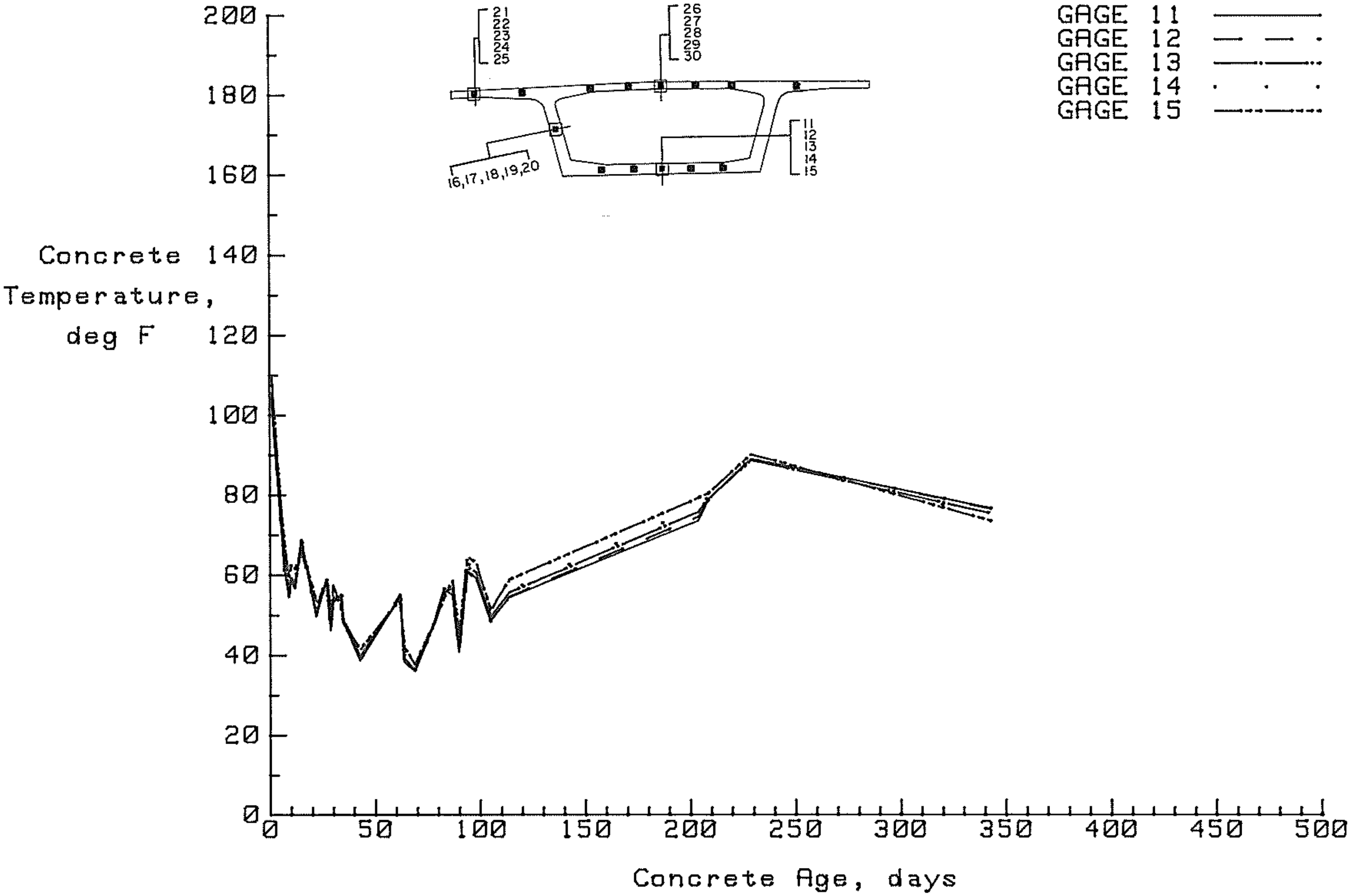

FIG. 5-25 THERMOCOUPLE READINGS FOR GAGES 11, 12, 13, 14, AND 15 OF SEGMENT 1313

Figure 50. Thermocouple readings for Gages 11, 12, 13, 14, and 15 of Segment 1313.

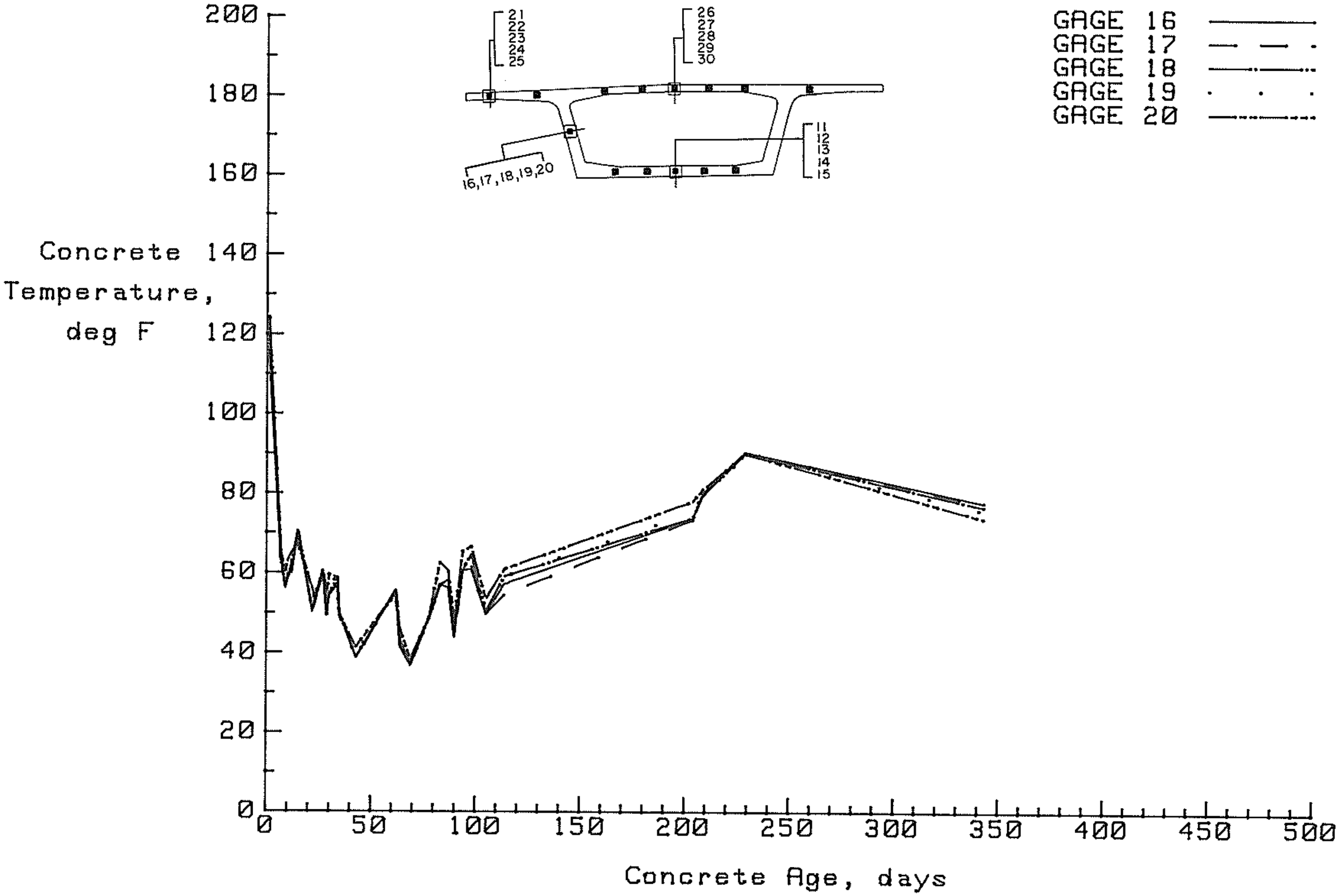

FIG. 5-26 THERMOCOUPLE READINGS FOR GAGES 16, 17, 18, 19, AND 20 OF SEGMENT 1313

Figure 51. Thermocouple readings for Gages 16, 17, 18, 19, and 20 of Segment 1313.

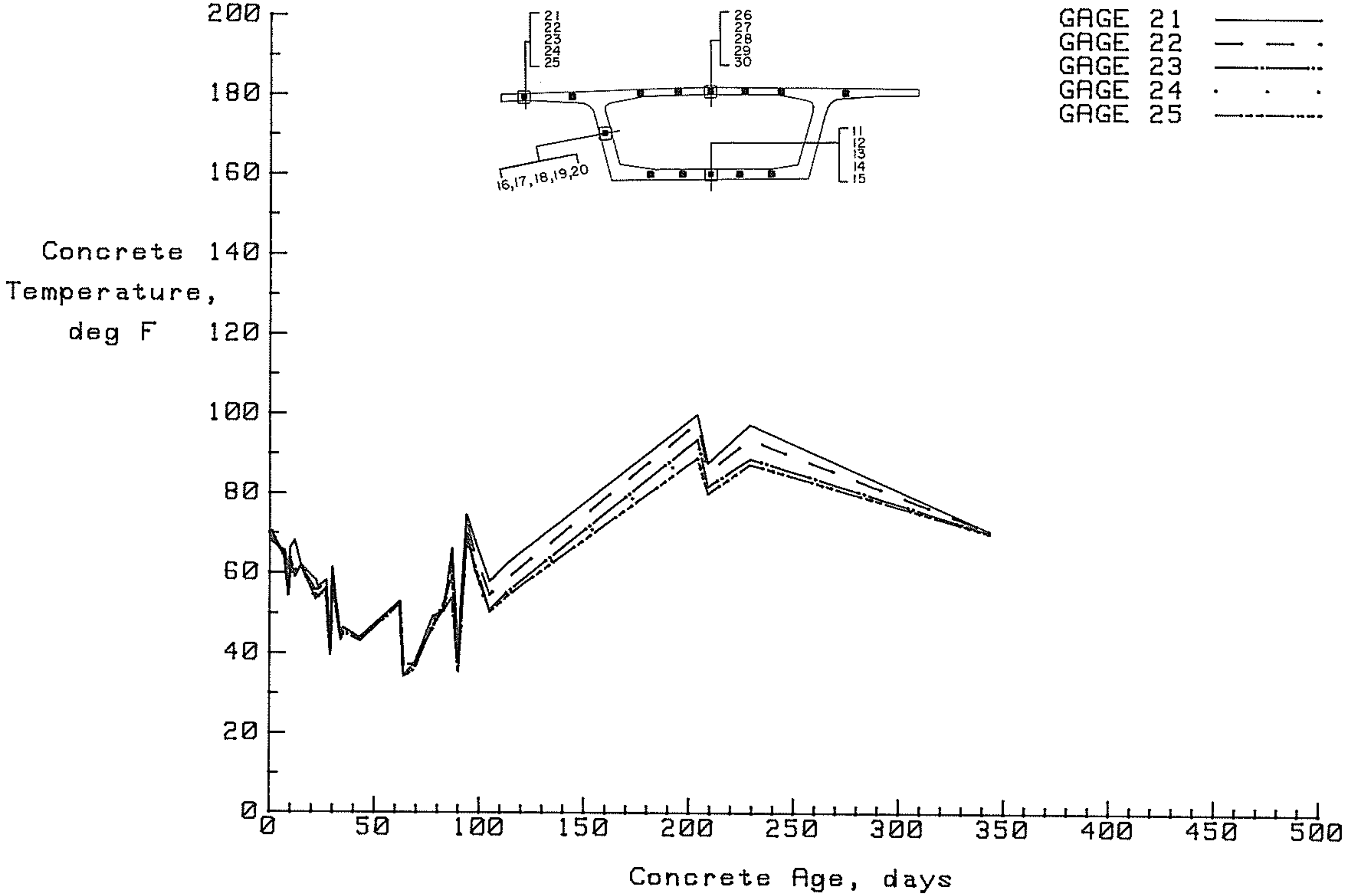

FIG. 5-27 THERMOCOUPLE READINGS FOR GAGES 21, 22, 23, 24, AND 25 OF SEGMENT 1313

Figure 52. Thermocouple readings for Gages 21, 22, 23, 24, and 25 of Segment 1313.

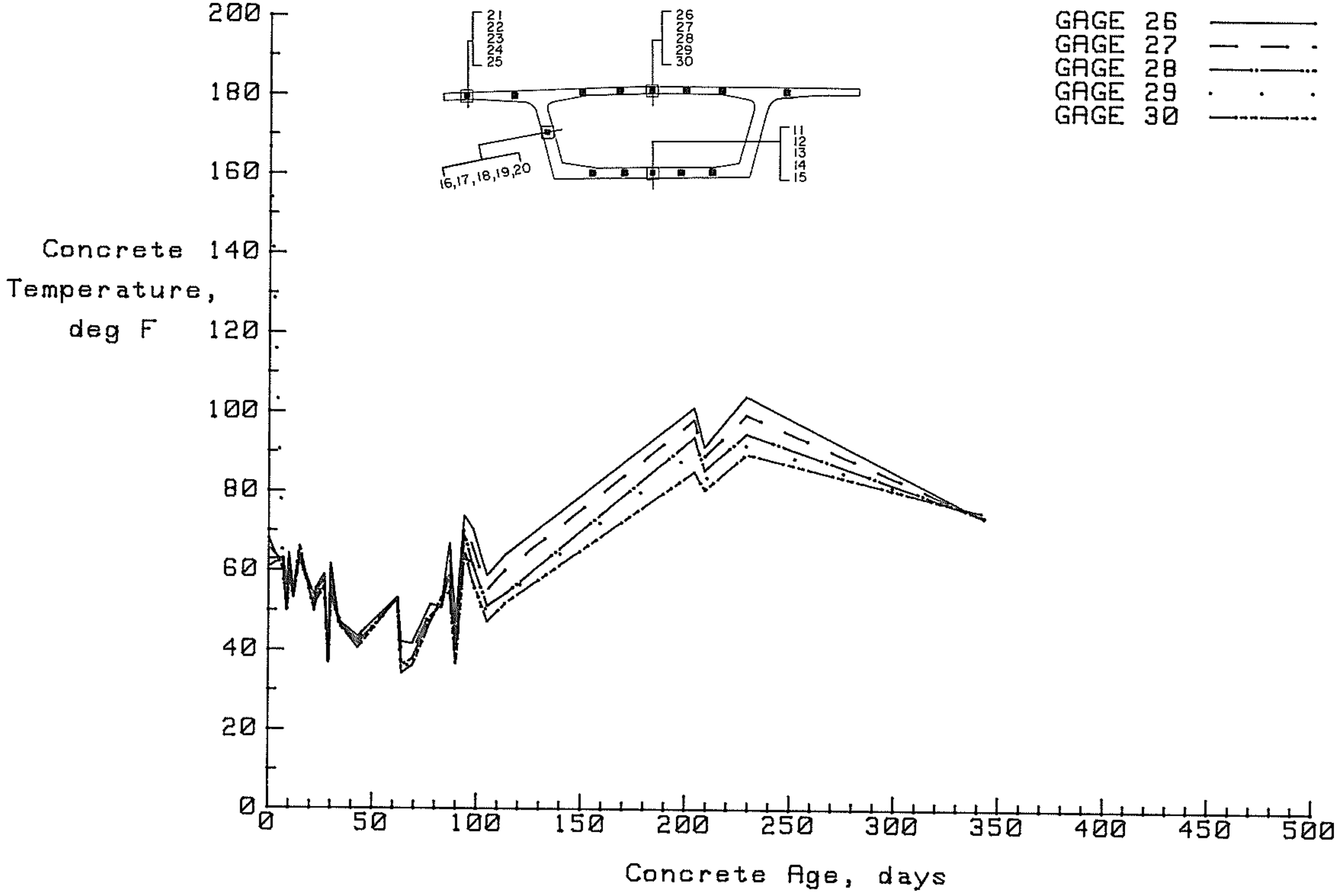

FIG. 5-28 THERMOCOUPLE READINGS FOR GAGES 26, 27, 28, 29, AND 30 OF SEGMENT 1313

Figure 53. Thermocouple readings for Gages 26, 27, 28, 29, and 30 of Segment 1313.

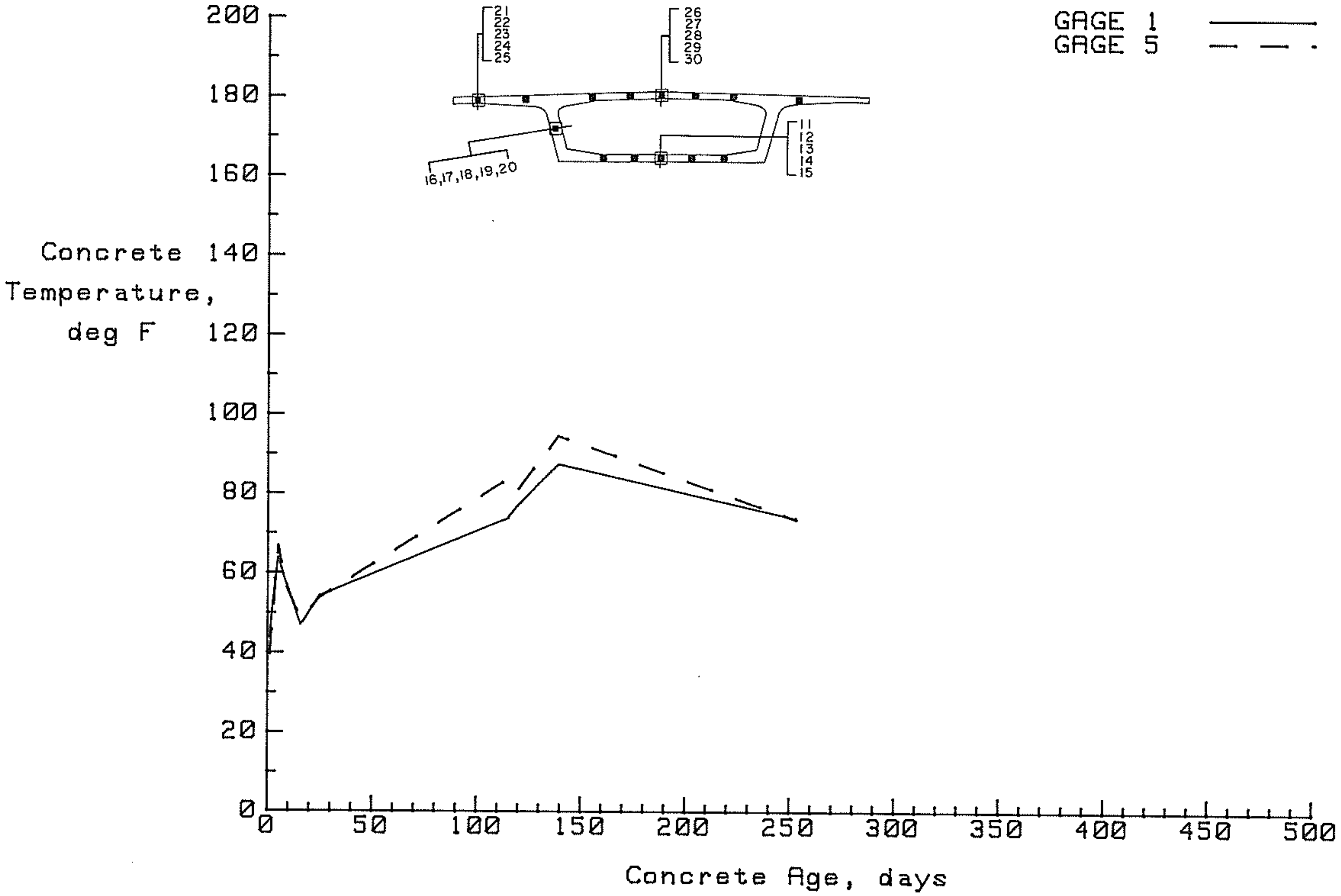

FIG. 5-29 THERMOCOUPLE READINGS FOR GAGES 1 AND 5 OF SEGMENT 1323

Figure 54. Thermocouple readings for Gages 1 and 5 of Segment 1323.

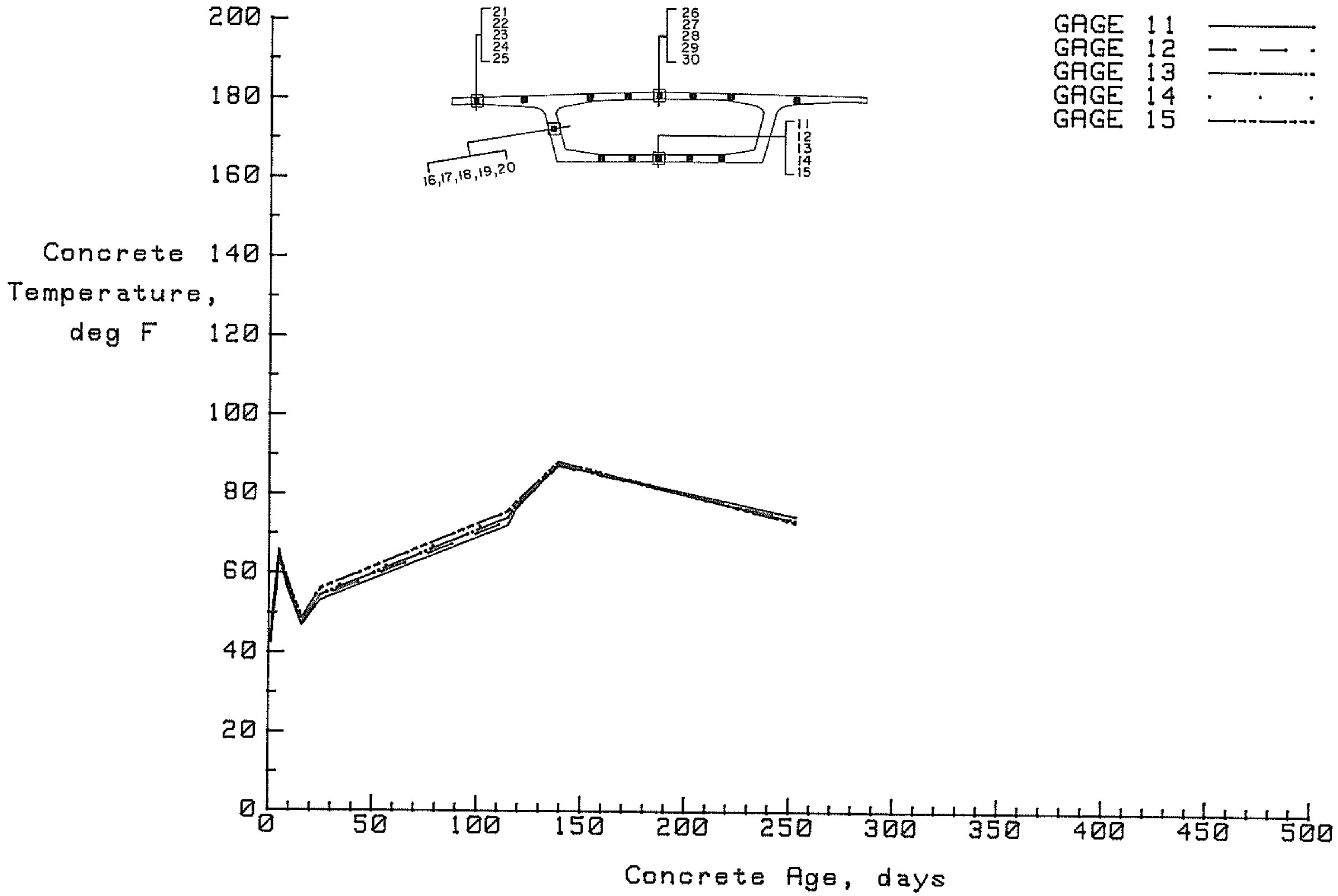

FIG. 5-30 THERMOCOUPLE READINGS FOR GAGES 11, 12, 13, 14, AND 15 OF SEGMENT 1323

Figure 55. Thermocouple readings for Gages 11, 12, 13, 14, and 15 of Segment 1323.

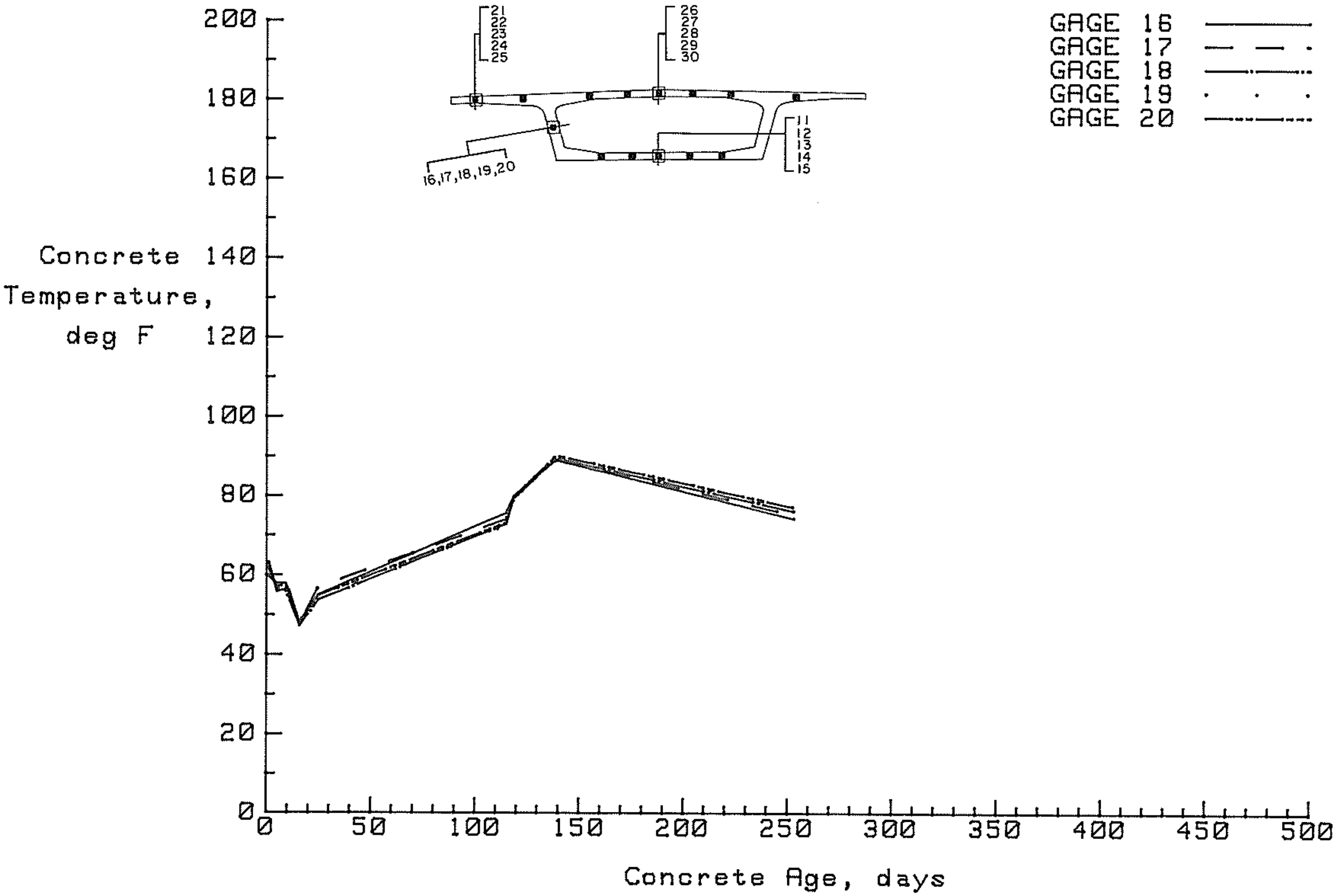

FIG. 5-31 THERMOCOUPLE READINGS FOR GAGES 16, 17, 18, 19, AND 20 OF SEGMENT 1323

Figure 56. Thermocouple readings for Gages 16, 17, 18, 19, and 20 of Segment 1323.

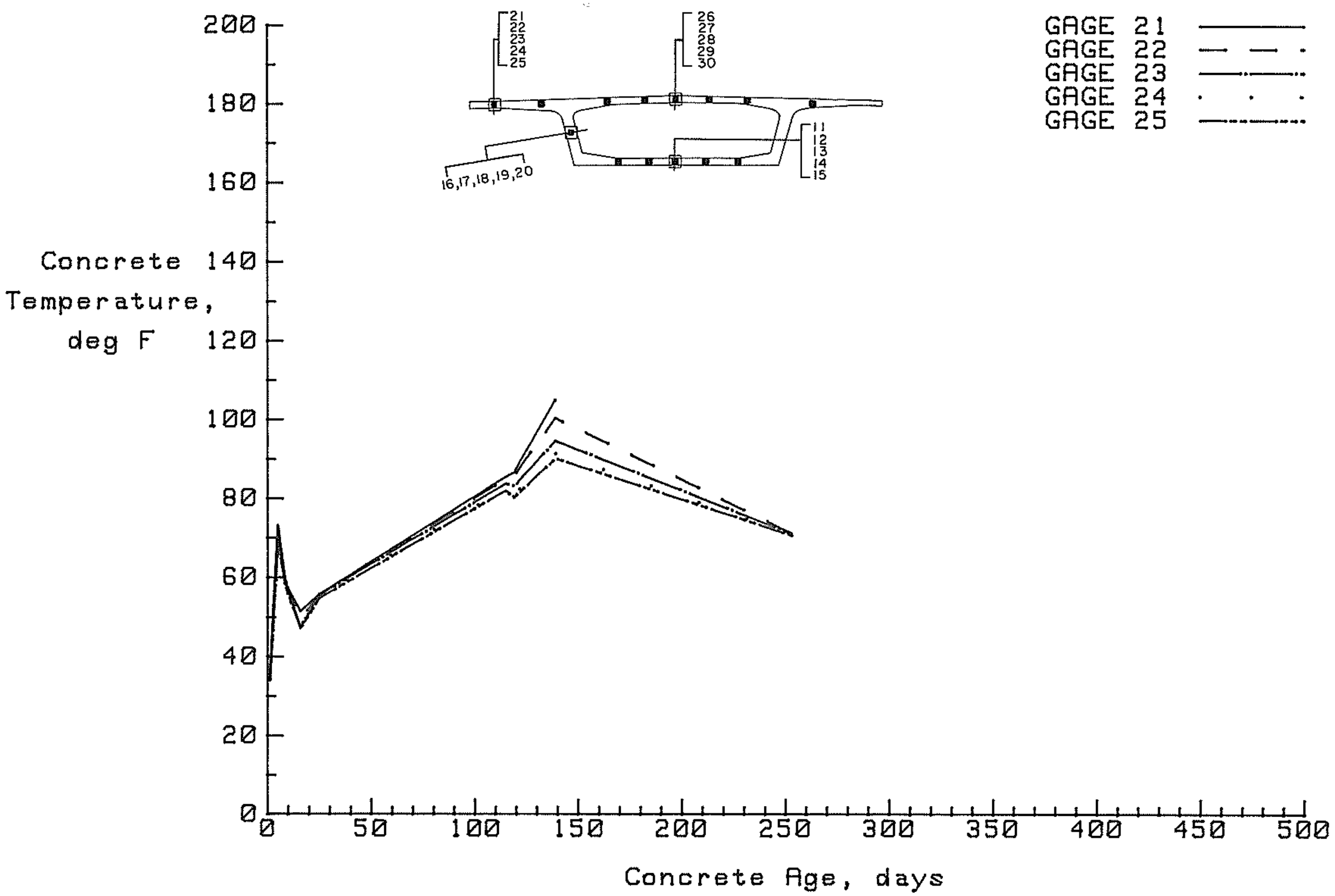

FIG. 5-32 THERMOCOUPLE READINGS FOR GAGES 21, 22, 23, 24, AND 25 OF SEGMENT 1323

Figure 57. Thermocouple readings for Gages 21, 22, 23, 24, and 25 of Segment 1323.